DEPARTAMENTO DE CIÊNCIAS DA VIDA

FACULDADE DE CIÊNCIAS E TECNOLOGIA
UNIVERSIDADE DE COIMBRA

Characterization of ELP3 as a Disease Modifier of Amyotrophic Lateral Sclerosis

Lara Aletta Gruijs da Silva

2015

Lara Aletta Gruijs da Silva Characterization of ELP3 as a Disease Modifier of Amyotrophic Lateral Sclerosis

DEPARTAMENTO DE CIÊNCIAS DA VIDA

FACULDADE DE CIÊNCIAS E TECNOLOGIA
UNIVERSIDADE DE COIMBRA

Characterization of ELP3 as a Disease Modifier of Amyotrophic Lateral Sclerosis

Dissertação apresentada à Universidade de Coimbra para cumprimento dos requisitos necessários à obtenção do grau de Mestre em Biologia Celular e Molecular, realizada sob a orientação científica do Doutor André Bento Abreu (Katholic University of Leuven) e do Professor Doutor Carlos Duarte (Universidade de Coimbra)

Lara Aletta Gruijs da Silva

2015

Versalius Research Center (VIB)

KU Leuven, Belgium

University of Coimbra

Faculty of Science and technology

Master of Cellular and Molecular Biology

Neurobiology specialization

Characterization of ELP3 as a disease modifier of Amyotrophic Lateral Sclerosis

Student: Lara Aletta Gruijs da Silva

Supervisor: André Bento Abreu
Promotor: Wim Robberecht

Internal Tutor: Carlos Duarte

2015

Acknowledgments

First of all I need to thank André for giving of his time, energy and expertise. Thank you very much for teaching me in the best way, I am a lot wiser thanks to that.

I also need to thank Pr. Dr. Wim Robberecht and Pr. Dr. Ludo Van Den Bosch for giving me the amazing opportunity to start this thesis and be part of the neurobiology Lab.

I am special grateful to my parents Aletta & Mário, and my brother Ivan who always support me in my decisions. Even far away you gave me unconditional emotional support, motivating me to keep on strong. I cannot forget to mention the rest of the family, thank you all for your dedication and care.

A special thanks to Ana's that were always there for the good and for the bad, even if for that we needed to cross countries. Oreo and Telmo for all the funny moments. Without you guys this journey would have not been so exceptional.

To my running buddy Louis for the contagious enthusiasm and all the help in and outside the Lab.

For the last but not less important I am grateful for all the assistance, advises and daily company of my lab colleges.

Leuven, June 2015

Lara Silva

Abstract

Amyotrophic lateral sclerosis (ALS) is the most common motor neuron disease in adults. It is a spontaneous and relentlessly progressive disease caused by motor neuron degeneration. Previous studies based on familiar ALS (FALS) cases have identified mutations in several genes, such as SOD1, C9orf72, TDP43 or FUS/TLS, which cause the characteristic phenotypes in ALS[2,4]. However, more recently, susceptibility to develop neurodegenerative disorders has been associated with genetic modulators. This disease modifiers are thought to modulate the phenotype induced by the causal genes. Elongator Protein 3 (ELP3), a subunit of the RNA elongator complex, was found to correlate with ALS[1]. This protein is required for RNA processing, as part of the RNA polymerase II complex. Besides its role in RNA elongation, it is also involved in tRNA wobble nucleosides modification[5,6]. The role of ELP3 on RNA biology suggests it can be an important feature in the pathophysiology of this neurodegenerative disease.

ELP3 role as an ALS modifier has not been investigated before, constituting the aim of this project. Therefore, modulation of ELP3 expression was investigated in the SOD1 mouse and in a C9orf72 repeat expansion zebrafish model. Additionally, the molecular mechanisms underlying the neuroprotective role of ELP3 were also assessed, with focus on ELP3 capacity to modify tRNAs at the wobble position.

The results show that overexpression of human ELP3 in the SOD1G93A mouse prolonged the survival. Moreover, in a C9orf72 zebrafish model, human ELP3 overexpression partially prevented the axonopathy induced by the 66x(G_4C_2) repeat expansion. Finally, the molecular mechanism underlying the ELP3 protective role still remains to be clarified, since the data obtained were inconclusive.

Keywords

Amyotrophic lateral sclerosis, neurodegeneration, pathogeneses, treatment, ELP3

Resumo

A Esclerose lateral amiotrófica (ALS) é a doença do neurónio motor mais comum em adultos. É uma doença progressiva espontânea e implacável causada por degeneração dos neurónios motores. Estudos anteriores baseados em casos de ALS familiar (FALS) identificaram mutações em diversos genes, entre eles o SOD1, C9orf72, TDP43 e FUS/TLS, que causam os fenótipos característicos da ALS. No entanto, mais recentemente, a suscetibilidade para o desenvolvimento de doenças neurodegenerativas foi associado a moduladores genéticos. Pensa-se que estes modificadores da doença irão modular o fenótipo induzido pelos genes causais. Foi encontrada uma relação entre a proteína de elongação *3* (ELP3), uma subunidade do complexo elongador de *RNA*, e a ALS. Esta proteína é necessária para o processamento do RNA, como parte do complexo de RNA polimerase II. Além do seu papel na elongação do RNA, está também envolvido na modificação *wobble* de nucleosídeos nos tRNA. A função do ELP3 na biologia do RNA sugere que poderá ser uma parte importante na fisiopatologia desta doença neurodegenerativa.

O papel da ELP3 na modificação da ALS não foi investigado anteriormente, sendo este o objetivo do presente trabalho. Deste modo, foi investigada a modulação da expressão do ELP3 no camundongo SOD1 e no modelo de peixe zebra C9orf72. Adicionalmente, foi testado também o mecanismo molecular subjacente ao papel neuroprotetor da ELP3, focando na capacidade da ELP3 de modificar tRNAs na posição *wobble*.

Os resultados revelam que a sobre-expressão da ELP3 humana no modelo SOD1 prolonga a sobrevivência. Adicionalmente, no modelo de peixes zebra C9orf72, a sobre-expressão da ELP3 humana previne parcialmente a axonopatia induzida pela expansão das repetições 66x(G_4C_2). Além do mais, o mecanismo molecular responsável pelo efeito protetor da ELP3 permanece ainda por clarificar, uma vez que os resultados obtidos foram inconclusivos.

Palavras-chave

Esclerose Lateral Amiotrófica, neurodegeneração, patologia, tratamento, ELP3

Abbreviations

AAV9	adeno-associated virus serotype 9
ALS	amyotrophic lateral sclerosis
AMPA	α-amino-3-hydroxy-5-methyl-4-isoxazoleproprionic acid
ANOVA	analysis of variance
ATP	adenosine triphosphate
Bcl-2	B-cell lymphoma 2
BSA	Bovine Serum Albumin
CAGG	cytomegalovirus immediate-early enhancer and chicken β–actin promoter/enhancer
C9orf72	chromosome 9 open reading frame 72
C9orf72 HNR	C9orf72 hexanucleotide repeats
CreER	Cre integrase and estrogen receptor fusion
DMSO	dimethyl sulfoxide
DNA	deoxyribonucleic acid
DPR	dipeptide repeat
Gln	glutamine
Glu	glutamic acid
HAT	histone acetyltransferase
EAAT-2	excitatory amino-acid transporter 2
ELP3	elongator protein 3
ER	endoplasmic reticulum
FALS	familial amyotrophic lateral sclerosis
FTLD	frontotemporal lobar degeneration
FUS/TLS	fused in sarcoma/translocated in Sarcoma
Gln	glutamine
Glu	glutamic acid
HSR	heat-shock response
hpf	hours post-fertilization
huELP3	human ELP3
kDa	kilodalton
Lys	lysine
mcm^5U	5-methoxycarbonylmethyl-uridine
$mcm^5s^2U_{34}$	5-methoxycarbonylmethyl-2-thio -uridine
Met	methionine
mRNA	messenger ribonucleic acid
ncm^5U	5-carbamoylmethyl-uridine
NMDA	ionotropic N-methyl-D-aspartate
NMJs	neuromuscular junctions
PAGE	polyacrylamide gel electrophorese
PBS	phosphate-buffered saline
PBST	PBS with 0.1 % Triton X-100

PCR	polymerase chain reaction
PFA	paraphormaldehyde
QGSY	glutamine, glycine, serine and tyrosine residues
RAN	repeat-associated non-ATG
RGG	arginine, glycine, glycine repeats
RIPA	radioimmunoprecipitation Assay
RNA	ribonucleic acid
RNAPII	RNA polymerase II
RRM	RNA-recognition motif
SALS	sporadic amyotrophic lateral sclerosis
SAM	s-adenosyl-methionine
SDS	sodium dodecyl sulphate
SEM	standard error of the mean
SOD1	superoxide dismutase 1
TBS	Tris-buffered saline
TDP-43	43 kDa TAR DNA-binding protein
tE	$tRNA^{Glu}_{UUC}$
Thy1	thymocyte antigen 1
tK	$tRNA^{Lys}_{UUU}$
tM	$tRNA^{Met}_{CAU}$
tQ	$tRNA^{Gln}_{UUG}$
T_m	melting temperature
Tris	2-amino-2-hydroxymethylpropane-1,3-diol
tRNA	transfer ribonucleic acid
Tx	tamoxifen
U	uridine

Index

1. Introduction

1.1. ALS – A neurodegenerative Disease

Amyotrophic lateral sclerosis (ALS) was first described in 1869 by Jean-Martin Charcot, a French neurobiologist[7]. Also known as Lou Gehrig's disease, it is the most recurrent motor neuron degenerative disorder, with an incidence of 1-2 cases per 100 000 individuals. The onset is around the age of 60 years and rarely appears in young people[4,8]. Male are more prone to be affected by the disease than female. The characteristic physical symptoms include muscle atrophy, spasticity, weakness and fasciculation, due to selective loss of motor neurons in the upper motor control (cerebral cortex) and/ or lower (brainstem and spinal cord ventral horn) centers[2].

Known as a progressive disorder, it is believe to affect first axonal connections, reaching then the cell body leading the motor neuron towards cell death[2], in a process known as "dying-back" mechanism. Normally patients only survive 2 to 5 years after disease onset[4], due to respiratory failure caused by denervation of the respiratory muscles.

The phenotype of ALS patients at onset is varied. About 70% of ALS cases are termed limb-onset ALS, where the combination of upper and lower motor neurons denervation leads to muscle dysfunction and consequent atrophy. Bulbar-onset (about 25% of ALS cases) can also occur, being presented by difficulties for swallowing and speech, with late limbic features onset. However, upper or lower motor neurons can be exclusively affected, known as primary lateral sclerosis[9].

1.2. ALS categories

Approximately 10% of the cases are familial (FALS), the rest being considered sporadic (SALS). Most familial incidences are autosomal dominant, while others less frequent are recessive and X-linked[2].

Presenting a similar phenotype, SALS patients do not show a familiar history of the disease, occasionally owing by misleading family data[2,4]. Mutated genes causing FALS have also been reported in SALS[10,11]. For example, positive inclusions regarding superoxide dismutase 1 (SOD1) and TAR DNA-binding protein 43 (TDP-43) have been found in the two types of ALS[12,13]; on another interesting finding, cerebrospinal fluid from both type of patients, induced similar toxic effects on *in vit*ro cultured rat spinal cord neurons[14]; finally, both FALS and SALS patients

respond in the same way to riluzole treatment[15]. SALS is also called as isolated ALS, where possible environmental and/or genetic causes can be involved, since this terminology of "sporadic" disease is, by definition, nongenetic[2].

Fifteen percent of the ALS patients are affected in prefrontal and temporal neurons, which result in frontal executive dysfunction and consequent frontal dementia[2,4], known as ALS with frontotemporal lobe degeneration (ALS/FTLD). FTLD pathology is greatly associated with TDP43 and FUS/TLS inclusions in cortical neurons, and motor neurons of patients with ALS. This findings support the idea that ALS and FTLD are related. The recent finding that an hexanucleotide repeat expansion on the C9orf72 gene causes both ALS and FTLD patients confirmed this idea and these two diseases are now considered part of a neurodegenerative disorder spectrum[16,17].

1.3. ALS pathogenesis

The mechanisms underlying the pathophysiological development of ALS seem to be multifactorial (figure 1), with strong evidence of genetic and molecular pathways snooping in this process[2].

Current hypothesis for these biological mechanisms converge a diverse range of cellular mechanisms that increase motor neurons vulnerability to degeneration.

Previous studies, have demonstrated that before motor neuron loss, protein-rich inclusions in the cell bodies and axons and aberrant RNA metabolism arises, which disrupt ordinary protein homeostasis and induce cellular stress[2,4]. Interfering with several cellular functions such as mitochondria metabolism, intracellular transport and cytoskeletal architecture[2].

In this context, there has been identified several responsible mutated genes, although few of them are linked with a significant percentage of ALS cases, but all have in common the capacity to contract motor neuron disorder even with a very heterogeneous range of biological functions (table 1)[2]. The most common mutations established in FALS are C9ORF72, SOD1, followed by FUS/TLS and TARDBP[10,18].

Table 1. **Amyotrophic lateral sclerosis associated genes (Adapted from Robberecht and Philips [2])**

Mutant molecule	Gene locus	Inheritance	Predominant phenotype					Estimated% of FALS	Refs
			ALS	ALS±FTLD	PLS	PMA	FTLD		
Enzyme									
Superoxide dismutase 1 (SOD1)	21q22.1	Dominant*	+	Rare		+		20%	231
RNA-binding and/or processing protein dysfunctions									
TAR DNA-binding protein 43 (TDP43)	1p36.2	Dominant	+	+			Rare	1–5%	49,50
FUS	16p11.2	Dominant	+‡	+			Rare	1–5%	84,87
TATA-binding protein associated factor 15 (TAF15)	17q11.1–q11.2	Unknown	+					Unknown	98
Ewing sarcoma breakpoint region 1 (EWSR1)	Unknown	Unknown	+					Unknown	99
Angiogenin (ANG)	14q11.2	Dominant	+	+				<1%	232
Senataxin (SETX)	9q34	Dominant	(+)§					Unknown	233
Repeat expansions									
Chromosome 9 open reading frame 72 (C9ORF72)	9p21.3–p13.3	Dominant	+	+			+	40–50%	107,108
Ataxin 2 (ATXN2)	12q24	Dominant	+			+		<1%	68
Proteostatic proteins									
Ubiquilin 2 (UBQLN2)	Xp11	Dominant		+				<1%	24
Optineurin (OPTN)	10p15–p14	Dominant‖	+	+				<1%	35
Sequestosome (SQSTM1)	5q35	Dominant	+	+			+	Unknown	29
Valosin-containing protein (VCP)	9p13	Dominant	+	+			+	<1%	30
Charged multivesicular body protein 2b (CHMP2B)	3p11	Dominant	+	+			+	Unknown	34
Phosphatidylinositol 3,5-bisphosphate 5-phosphatase (encoded by *FIG4*)	6q21	Dominant	+		+			Unknown	36
Excitotoxicity									
D-amino-acid oxidase (DAO)	12q24	Dominant	+					<1%	146
Cytoskeleton/cellular transport deficits									
Vesicle-associated membrane protein-associated protein B and C (VAPB)	20q13.3	Dominant	+		+	+		<1%	184
Peripherin	12q13.12	Sporadic	+					Unknown	176
Dynactin 1 (DCTN1)	2p13	Dominant	+					Unknown	180
Neurofilament heavy chain (NFH)	22q12.2	Dominant?	+					Unknown	177
Profilin 1 (PFN1)	17p13.2	Dominant	+					Unknown	181
Uncertain									
Spatacsin	15q21.1	Recessive	+‡					Unknown	234
Alsin	2q33.2	Recessive	+‡		+			<1%	185,235
Awaits identification	18q21	Dominant	+					Unknown	236
Awaits identification	20ptel–p13	Dominant	+					Unknown	237
Awaits identification	15q15.1–q21.1	Recessive	+					Unknown	238

ALS, amyotrophic lateral sclerosis; FALS, familial ALS; FTLD, frontotemporal lobe degeneration; NA, not applicable; PLS, primary lateral sclerosis; PMA, progressive muscular atrophy. *Recessive for D90A in Scandinavian population. ‡Juvenile onset possible. §Phenotype more similar to Silver syndrome than to ALS. ‖May be recessive in Japanese population.

1.3.1. C9orf72 mutations and RNA toxicity

A hexanucleotide repeat expansion on C9orf72 is the cause of almost 50% of FALS and about 7% of SALS, accounting for the most significant proportion of the ALS cases. The mutation that occurs is an expantion of the GGGGCC hexanucleotide-repeat, a sequence that is located between exons 1a and 1b. In normal conditions, individuals have less than 30 repeat, while in ALS patients repeats are up to thousands. This expansion is also reported in FTLD patients that do not carry ALS. The existence of a common genetic etiology between ALS and FTD suggest C9orf72 as a common genetic factor that can cause either condition[2,10,19,20]. In ALS

this mutation is reported to be associated with bulbar onset and a frontotemporal involvement. Psychosis, ataxia and Parkinsonism can also be part of its clinical features, when talking about an adult-onset. Some ALS patients who carry C9orf72 hexanucleotide expansions report typical features of ALS with TDP43-positive inclusions in the remaining cortex and hippocampal motor neurons[21].

C9orf72 HNR carriers are associated with a characteristic pathogenic feature. TDP-43-positive neuronal cytoplasmic inclusions and glial cytoplasmic inclusions are typical to be found in the motor cortex and anterior horns of the spinal cord of these patients, additionally to the massive loss of motor neurons[22]. However similar to other subtypes of ALS, here this inclusions were also found in extramotor regions, not predicted to be affected in ALS as in the hippocampal pyramidal cells[23,24].

C9orf72 is an uncharacterized protein and the way its repeat expansion mutation contributes to neurodegeneration is unclear. However, knowledge from other repeat expansion diseases such as spinocerebellar ataxia type 8 and myotonic dystrophy type 1, suggest three potential pathogenic mechanism that can be associated with C9orf72 mutations: haploinsufficiency; toxic RNA gain of function by sequestration of RNA binding proteins to transcripts with expanded repeats; and toxicity of products generated by unconventional repeat-associated non-ATG (RAN) translation of transcripts with expanded repeats[2,19,21,25].

In patients with a C9orf72 expansion, reduction of C9orf72 mRNA has been showed[16]. These findings suggested a loss-of-function mutation in which the expanded allele does not give rise to mature mRNA. As ALS caused by C9orf72 mutations is dominantly inherited, one allele therefore has to invoke haplo-insufficiency[2]. However, more recent studies report that this finding is not consistent[26]. For example, was demonstrated that expansions around 50 HNR do not show this reduction in transcription of C9orf72[27]. Additionally, 2 patients carrying the both C9orf72 loci expansions, but one being homozygote and the other heterozygote, did not express differences in phenotype severity spectrum, what would be expected in a haploinsufficiency model, where severity would be dependent from the number of involved alleles[27,28].

In C9orf72 repeat expansion carriers occurs an abnormal recruitment of splice factors, RNA-binding proteins which bind to the repeat expansion, leading to the formation of RNA foci[16]. A possible mechanism of toxicity can result from the formation of aberrant splicing of diverse genes, generating transcripts missing exons that are intended to be retained or containing exons that are meant to be spliced out. Consequently, sequestration of certain proteins can produce nuclear stress and increased susceptibility to excitotoxicity can occur[29]. This increase attraction of the RNA-binding proteins to the repeats, can additionally unable its

recruitment for current spicing of other mRNAs, such as Tau and troponin, since these splicing factors are not available, resulting in the expression of abnormal proteins[2,30].

Moreover, the expansion is also associated with the formation of insoluble and potentially toxic dipeptide repeat (DPR) proteins through repeat-associated non-ATG (RAN) translation, which happens across long, hairpin-forming repeats. However, the pathogenic implication of these DPR proteins still needs to be validated[2,21,31].

1.3.2. SOD1 mutations induced toxicity

Mutations in Cu/Zn superoxide dismutase (SOD1) is one of the most frequent cause of inherent ALS, underlying approximately 20% of the cases[2]. Its association with ALS was establish in 1993, when a missense mutation in SOD1 gene (chromosome 21) was discovered in families carrying ALS[32]. Currently, more than 150 mutations, dispersed through the five exons that encodes for the 153-amino-acid SOD1 protein, were reported to be associated with the pathogenesis[10,33,34]. Barely any are recessive mutations, such as the D90A mutation[2,35], are rare and were reported in the Scandinavian population.

SOD1, an ubiquitous enzyme, is expressed in the cytoplasm. It has a role in free radical scavenging, catalyzing the dismutation of superoxide anions to hydrogen peroxide, which can be later on cleared to oxygen and water[36]. Regarding its catalytic activity, it was initially though that mutated SOD1 pathogenesis in ALS was due to the accumulation of toxic superoxide radicals in motor neurons[32]. However, the progressive symptoms, like muscle weakness and premature death in transgenic mice expressing inherent ALS-linked mutant SOD1[37-41], showed that toxic effects, progressive motor neuron junctions retraction, impaired mitochondria activity, microglia activation and consequent motor neuron degeneration occurs despite increasing SOD1 enzymatic activity[38,41-43]. Additionally, mice that do not express SOD1 gene showed no motor neuron disease propensity[44], strengthening the idea that the simple loss-of-function of SOD1 is not the cause for its role in ALS pathology.

As in other neurodegenerative disorders (Alzheimer, Parkinson and Huntington), ALS shows as pathological hallmark the presence of cytoplasmic protein aggregates. The hypothesis for mutated SOD1 molecular pathology is related to its capacity to aggregate. Chaperon folding system and degradation proteasome pathway show to be impaired in mutant SOD1 mice, which together may overload misfolding and accumulation of this insoluble form of the protein, which lead to a stress response[45]. Therefore, increasing accumulation of mutated SOD1 oligomers and additional stressors (age) will induce an unfolded protein response. This will interfere with several functions in the cell. For example,

interaction of the oligomers with other proteins can occur, disrupting their function and axonal transport, by the formation of intracellular inclusions. Other target can also be mitochondria, disrupting cell energy production[46].

1.3.3. TDP-43 and FUS/TLS mutations and RNA processing

Some proteins involved directly and indirectly in RNA processing show to be associated with ALS[10,47]. In this context, two specific proteins, TDP43 and RNA-binding protein FUS, involved in pre-mRNA splicing, RNA transport and translation were identified to be mutated.

TDP43 protein is coded by TARDBP gene, where mutations are preferentially located in exon 6, place that encodes for the glycine-rich domain in the protein C-terminal important to target RNA. Most of the mutations are missense, although there are some deletion mutations[10]. This protein belongs to a heterogeneous ribonucleoproteins family, and is found mainly in the nucleus where, together with other factors, is vital for proper RNA processing, interfering with transcription, RNA splicing and transport. However, the RNA splicing machinery carried by TDP43 seems to be of great importance[48,49]. Once TDP43 is knockdown, more than 965 mRNAs are affected by its unsuitable splicing. The failure in mRNA spicing results when TDP43 is mutated and tend to leave the nucleus, migrating to the cytoplasm where it accumulates into stress granules by its prion-like domain. This domain act as a template that induce the conversion of natively folded proteins, trapping the normal protein into the aggregate. Then RNAs fate can be degradation, formation of aberrant protein sequences or even be sequestered in the TDP43 accumulations, what can contribute to cytoplasm toxicity. Conclusively, TDP43 nuclear depletion and consequent cytoplasm aggregation induces abnormal RNA processing, following a loss-of-function mechanism responsible for ALS pathology[50].

Like TDP43, FUS/TLS is an RNA-binding protein that belongs to FET family. It is mutated in ALS, in a dominant form. The gene encoding FUS/TLS is located in chromosome 16, and mutations in this gene are responsible for 4-5% of FALS cases, less than 1% of all ALS cases. Also known as hnRNPP2, FUS/TLS is constituted by a prion domain, established by the N-terminal region rich in glutamine, glycine, serine and tyrosine residues (QGSY region) together with glycine-rich domain, which is essential for its capacity to aggregate[51,52]. It also contains an RNA-binding domain, consisting of multiple arginine, glycine, glycine (RGG) repeats and an RNA-recognition motif (RRM)[4]. Studies revealed that the mutant form of FUS/TLS is an insoluble protein that tend to accumulate into aggregates in the cytoplasm of neurons.

Specific mutations in FUS are linked with an aggressive phenotype of ALS, characteristic to be present during youth, when patients have between 10 to 20 years, surviving only 1 or 2 years[53-55].

In normal conditions FUS/TLS is mainly expressed in the nucleus, but it can also be found in dendrites, more precisely at the spines of excitatory synapses. Previous research regarding FUS/TLS deletion, showed that spine density decrease, whereas spine morphology is likely to be abnormal[56].

FUS targets seem to be different than those of TDP43. It is known that FUS is also involved in RNA splicing, but it also plays in the exportation of processed mRNA from the nucleus to the cytoplasm and acts as a detector of DNA damage, serving as a transcriptional regulator by repressing specific genes during transcription[57]. On the other hand, the role of mutated FUS/TLS in ALS is still an incognita, as it can be due to its loss of RNA processing function or its aggregative toxic function[4].

1.3.4. Non-cell autonomous neurodegeneration

Several types of non-neuronal cells, such as astrocytes and microglia, have also a direct contribution in ALS neurodegenerative process. Experiments in mutant SOD1 mice reveled that motor neuron death is not a cell autonomous process, as an increase activation of astrocytes and microglial cells that surround these neurons contribute to disease onset and progression[58].

The mechanisms underlying glial cell role in neurodegeneration progression seems to be related with the insufficient release of neurotrophic factors, the activation of neuroinflammatory response, the secretion of neurotoxic mediators and the failure in modulate glutamate receptor expression[2,59].

1.3.5. Excitotoxicity

Glutamate-induced excitotoxicity has been identified as a pathological evidence in ALS[60]. In the CNS, glutamate is the main excitatory neurotransmitter, activating ionotropic N-methyl-D-aspartate (NMDA) receptors and α-amino-3-hydroxy-5-methyl-4-isoxazoleproprionic acid (AMPA) receptors on the postsynaptic membrane, resulting in the influx of calcium and sodium in the postsynaptic neuron[60].

In pathological circumstances, over activation of calcium dependent enzymatic pathways, in response to excessive glutamate synaptic levels and/or increase in the

postsynaptic neuron sensibility to glutamate stimuli, lead to excitotoxicity and consequent neuronal death[60]. In this process, generation of free radicals can also be a consequence for glutamate-induced excitotoxicity, which in turn can induce the damage of intracellular organelles and activate inflammatory response prompt this neurons to neurodegeneration[61,62]. Other cellular dysfunctions can result also from this excitotoxicity phenomenon, like axonal transport disruption, mitochondria and sodium/calcium ion pump dysfunction.

Astrocytes play an important role in excitotoxicity. ALS patients have shown decreased levels of glial transport for glutamate (EAAT-2), resulting in defective glutamate synaptic clearance, once this is the main way to remove glutamate from the synaptic cleft. So, this can be one of the mechanism that prone motor neurons to injury through the increase in extracellular levels of glutamate[4]. Riluzole, a drug that promotes clearance of glutamate from the synaptic cleft, remains the only approved drug for the treatment of ALS.

1.3.6. Mitochondria dysfunction

A common feature of many neurodegenerative diseases is mitochondria dysfunction. Mitochondrial abnormalities, especially vacuolization and swelling are observed in the motor neurons of $SOD1^{G37R}$ mice, in early and pre-symptomatic stages of ALS. Mutant SOD1 in affected tissues is imported into mitochondria and several mechanisms have been suggested for its mediated damage to mitochondria[8].

First, it may interfere with the elements of the electron transport chain, disrupting ATP-generating oxidative phosphorylation. Then, mutant SOD1 may also impair calcium buffering mechanisms which buffer cytosolic calcium levels, and may indirectly affect similar pathways linked to mitochondria by physically blocking the protein import machines, TOM and TIM. Additionally, mutant SOD1 aggregates can also interfere with mitochondrial-dependent apoptotic machinery, such as Bcl-2, and consequent cytochrome c release into the cytosol, which thereby triggers premature activation of the apoptotic cascade. Finally, the oxidative damage carried by many mitochondrial proteins can also contribute to overall mitochondrial dysfunction. Taking all of these mechanisms in consideration, disruption of motor neurons homeostasis can be predicted, which ultimately can trigger motor neuron death[7,8].

1.3.7. Compromised axonal transport in ALS

Motor neurons in ALS are characterized to present aberrant accumulations of neurofilaments in their cell body and proximal axons. Known to be critical for axonal growth, neurofilaments are the most abundant cytoskeletal protein present in large myelinated axons. Transgenic mice carrying point mutations or overexpressing neurofilament subunits display selective motor neuron dysfunction by neurofilament accumulation[7].

Decreasing axonal neurofilaments in SOD1 mice substantially prolongs mice survival. Hence, decreasing the axonal burden of neurofilaments may protect motor neurons by enhancing axonal transport[10].

Furthermore, the identification of a point mutation in the gene encoding dynactin, supports the link between motor neuron degeneration and axonal transport. Dynactin is a protein involved in retrograde transport. Mutations were found in a family with an autosomal dominant form of lower motor neuron disease[7,10].

The mechanisms underlying motor neuron death by axonal transport failure are not clear but can include improper transport of mitochondria thought the axons and/or by inefficient deliver by retrograde transport of peripheral derived trophic factors[7].

1.3.8. Proteasome failure

In ALS one hypothesis regarding the contribution of aggregates to motor neuron toxicity, include aggregate-mediated inhibition of the proteasome machinery. Aggregates found in ALS patients, as well as mouse models, contain ubiquitin, a protein required to target proteins via the proteasome degradation pathway. The misaccumulation of ubiquitinated misfolded proteins might badly affect the proteasome machinery and consequently impair normal proteasome degradation. Actually, aggregates of SOD1 are dependent on proteasome activity. However, if dysfunction of proteasome activity is a cause or a consequence of aggregates formation is still unknown, due to reported contradictory results[7].

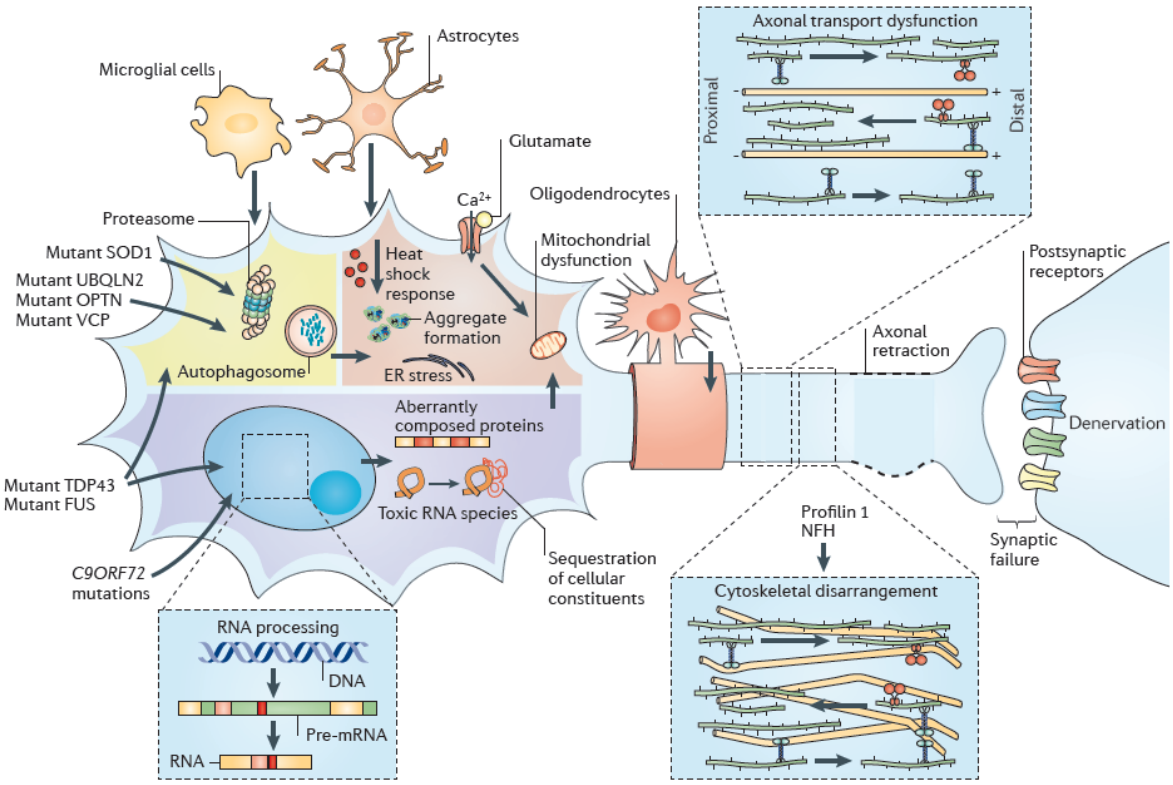

Figure 1. **Schematic synopsis of ALS pathogenesis. Mechanisms involved in ALS motor neuron degeneration, such as: mutated ALS genes induce proteasome dysfunction, heat-shock response (HSR), ER stress and consequent misfolded proteins aggregation, leading to cell toxicity, impaired axonal transport and mitochondria energy failure; RNA processing disruption, triggering toxic RNA species formation and assembling of deficient proteins; and increased in excitotoxicity, which together with the other disrupted cell functions play a central role in motor neuron death. (Adapted from Robberecht and Philips [2]).**

1.4. Elongator protein 3 (ELP3) and ALS

Motor neuron injury in ALS is persistently progressive, presenting a gradual spread. Although it is fatal after 2-5 years after onset, it has been observed that patients with the same mutation on an ALS causing gene can display the initial symptoms of the disease at different times and present heterogeneous length progression and consequent survival. This large variability in survival and time of onset, suggest the existence of modifying factors that can explain this heterogeneity[2].

A genome-wide association study in sporadic ALS patients identified ELP3 to correlate with the disease. Lower expression of ELP3 in the brain was associated with the presence of the at-risk allele. Moreover, in an independent screen in drosophila, two different loss-of-function mutations in the homologue of ELP3 were identified to induce synaptic defects. Furthermore, in the same study, abnormalities in motor axons were induced after knocking-down ELP3 in the zebrafish (figure 2). A recent publication based on C9orf72 HNR carriers, the major genetic cause in ALS, came to emphasize the importance of ELP3 in motor neuron disorders, showing that different variants of ELP3 display significant influence in disease onset and progression[63]. These findings suggest an essential role of ELP3 in the control of neurodegeneration progression. When its expression decreases it renders motor neurons vulnerable to neurodegeneration, whereas its increase may be neuroprotective[1].

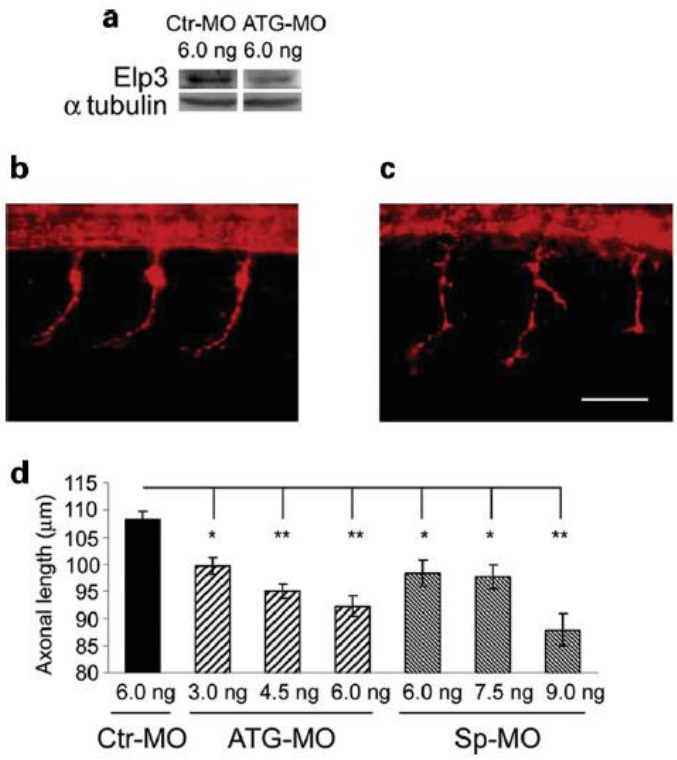

Figure 2. **Morpholinos-induced knock-down of ELP3 in Zebrafish model. (**A**) Western blot presenting the decrease levels of ELP3 after morpholino injection (ATG-MO). (**B;C**) ELP3 knockdown resulted in abnormal branching and decreased axonal length, respectively, compared with the controls (left) (Adapted from Simpson, et al. [1]).**

1.5. Elongator complex and transcription

ELP3 is part of Elongator complex, termed holo-Elongator, an unstable six-subunit complex (ELP1-ELP6). Elongator was discovered in yeast, to which Human elongator show a remarkable similarity, and it can be found as two discrete three-subunit complex[64]. One of these subcomplexes is the ELP3-containing core Elongator complex (ELP1, ELP2, and ELP3), and the other complex is composed of the ELP4, ELP5 and ELP6 proteins[5]. Protein ELP1 is the scaffold protein necessary to bring together all the subunits, required for a functional complex[64].

Holo-Elongator showed to associate with the hyperphosphorylated carboxy-terminal domain of RNA polymerase II (RNAPII)[65]. This association capacity suggested that Elongator complex assists RNAPII during chromatin remodeling, regulating transcription elongation (figure 4)[65,66].

The complex is indeed capable of acetylating histones, in which ELP3 is an essential element. ELP3 C-terminal domain has characteristics of the GCN5 family of histone acetyltransferase (HAT) domain. The HAT domain of ELP3 is known to acetylate histones, in particularly H3 lysine (Lys) 14 and H4 Lys8[6,67]. However, this HAT activity is inactive in core Elongator (ELP1/ELP2/ELP3) complex when the Holo-Elongator complex is not formed, indicating that the other components (ELP4, ELP5and ELP6) of the complex are required for proper catalytic activation. Moreover, neither ELP4, EPL5 nor ELP6 contain HATs motifs, consequently no HAT activity exists in the complex of these proteins[64].

ELP3 has also a N-terminal domain that uses S-adenosyl-methionine (SAM) to transfer monocarbon groups (mainly methyl groups) and it has been implicated in DNA demethylation of mouse zygotes[68].

1.6. ELP3 and tRNA modification

Previous studies provided new insight in the way the Elongator complex activity influences translation efficiency (figure 4). They show that this modulation is mediated by post-transcriptional nucleoside modifications in the anticodon loop of some tRNAs[6,69]. Transfer RNAs (tRNA) are adaptor molecules responsible for translation of mRNA into protein. These molecules require modifications at their nucleosides to optimize its function[70].

Wobble modifications is one of the 91 tRNA modifications found so far[70]. This modification occurs especially in tRNAs carrying a uridine at position 34 of the anticodon (wobble position). They have been shown to play a vital role in numerous processes e.g.,

increasing in codon recognition and efficiency[71-73], aminoacyl-tRNA synthetase interaction[71], or increasing translation fidelity by helping to bind only to the correct codon, by avoiding frame shifts[74,75].

Only thirteen tRNAs contain a uridine at the wobble position, eleven undergo a wobble modification 5-carbamoylmethyl-uridine (ncm^5U) or a 5-methoxycarbonylmethyl-uridine (mcm^5U), while three of the mcm^5 containing tRNAs, those coding for lysine (Lys), glutamine (Gln) and glutamic acid (Glu) undergoes a dual modification of uridines at position 34 (U_{34}) forming UUB anticodons ("B" being C, G or U)[6,66], in the addition to the methoxycarbonylmethyl at the carbon 5 of U they are thiolated at carbon 2, leading to the hyper modified 5-methoxycarbonylmethyl-2-thio -uridine ($mcm^5s^2U_{34}$)(figure 3)[76].

There are three possibilities for decoding that an aminoacyl-tRNA can proceed: Cognate codon, that follows Watson-Crick base pairs; Near-cognate codons, with two Watson-Crick base pairs and one wobble base pair at the third position; and Non-cognate codon: one or less Watson-Crick base pair[77]. An unmodified tRNA will recognize all four nucleotides U, C, A and G, whereas a modified uridine can alter this decoding capacity[78-80]. Was suggested that modified wobble tRNAs prevent pairing with U- and C- ending codons, and efficient reading of both A- and G- ending codons[79,81,82].

ELP3 gene showed to be necessary for this side chain formation at an early step synthesizing mcm^5 and ncm^5 groups at the wobble position[69,83-85].

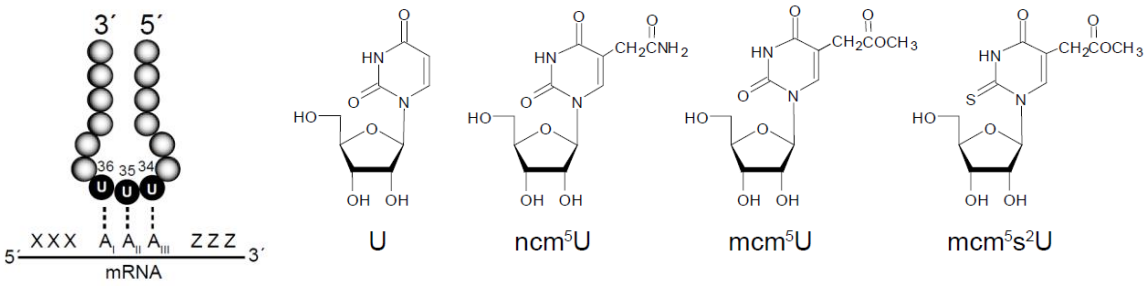

Figure 3. **In the right a schematic drawing of codon-anticodon interaction. The anticodon of the tRNA is composed of three nucleotides at position 34, 35, and 36 in which U34 (wobble base) is the third-position (AIII) of the mRNA codon. In the left examples of uridine or uridine modified at the 34 wobble position. From the left: uridine (U), 5-carbamoylmethyl-uridine (ncm5U), 5-methoxycarbonylmethyl-uridine (mcm5U), and 5-methoxycarbonylmethyl-2-thio -uridine (mcm5s2U) (Adapted from Chen, et al. [3]).**

Overexpression of two of these modified Elongator dependent tRNAs showed to rescue under stress yeast phenotypes (slow growth at 30°C; temperature-sensitive growth at 38°C) when Elp3 is not present. Therefore, $tRNA^{Lys}_{UUU}$ (tK) and $tRNA^{Glu}_{UUC}$ (tQ) which rescues the effect on Epl3 mutation suggest that the inability to modify these tRNA species are the main cause for the defects observed when Elp3 is deleted[6,69,85].

The contribution of ELP3 in tRNA modification seems indeed to be important to support stress conditions, causing inefficient mRNAs translation to occur in an ELP3-deficient yeast strain. One example is the deficient expression of the transcription factors Atf1 and Pcr1, which in normal conditions are induced by different stresses[6,86,87]. The codon usage of these genes are mainly AAA, which require the $tRNA^{Lys}_{UUU}$ (tK) decoding for translation. As tK is not that abundant in yeast, the evolutionary adaptation of its wobble modification, made it possible to be more specific for AAA codons[82]. Consequently, efficient translation of these AAA codon rich stress-induced highly expressed mRNAs is possible[6].

Thus, in stress conditions, modified nucleosides favors codon recognition, and therefore increase translation efficiency, fidelity and consequently organism viability[6].

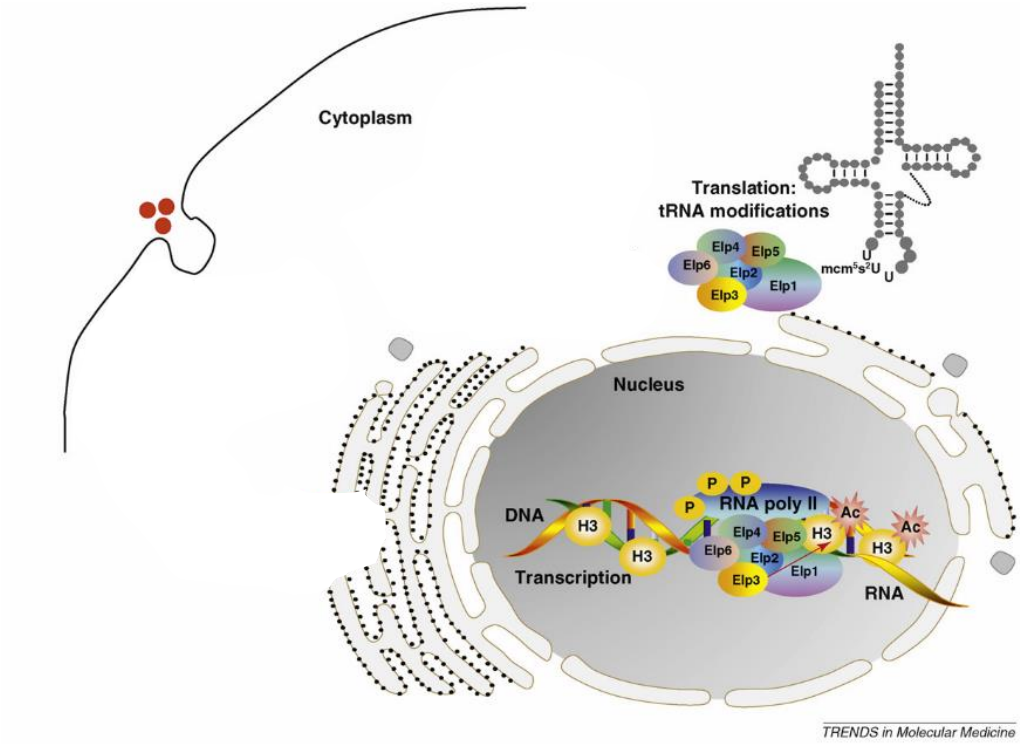

Figure 4. **Biomolecular mechanisms played by Elongator complex. The six subunit complex is required in the nucleus for RNA polymerase II hyperphosphorylation and for histone H3 acetylation, controlling the transcription of multiple genes. Additionally, in the cytoplasm, it regulates tRNA wobble modifications, regulating protein translation (Adapted from Nguyen, et al. [5]).**

1.7. Neuroprotective role of ELP3 in ALS

The best performance of a biological process such as cellular adaptation to environmental alterations requires that a complex phenomenon as protein expression to be supported with high efficiency and fidelity. So, not only transcription but also mRNA homeostasis and translation need to be achieved with maximum efficiency and fidelity and as mention above, ELP3 is an important protein required to ensure proper maintenance of these mechanisms[5,64,66].

Recently, an interesting study showed that ELP3 is essential for efficient translation of highly expressed stress-induced mRNAs, in particular the stress response transcription factors Atf1 and Pcr1, which are underexpressed in yeast lacking ELP3 after stress[6]. It suggests a possible reason why lower levels of ELP3 might increase the vulnerability of motor neurons in ALS models, as described above[1].

Nonetheless, recent experiments in Dr. Robberecht's lab have shown that deletion of ELP3 induces abnormalities of the active zone protein Bruchpilot directly, a protein required for the clustering of presynaptic calcium channels to ensure efficient vesicle release[88]. Furthermore, studies in this lab where already performed to study the effect of ELP3 deletion in the mouse. They generated an ELP3 knockout mouse (ELP3-/-), in which the homozygous form was not viable, dying around embryonic day 10, like the ELP1-/- mouse. Surprisingly, the heterozygous mouse (ELP3+/-) is phenotypically normal.

Moreover, they found that ELP3 is neuroprotective in zebrafish ALS models and also in the ALS mouse model. The protective effect of ELP3 was tested in the mutant SOD1, preventing motor axonopathy in this models (figure 5). The study regarding ELP3 overexpression in the SOD1G93A mouse, an ALS model, show preliminary evidence that ELP3 overexpression is neuroprotective, delaying disease onset and prolonging survival of these mice (figure 6). In this experiment, ELP3 overexpression was achieved by intrathecal delivery of AAV9-ELP3 viral particles in neonatal mice.

However, the viral ELP3 overexpression has some limitations, such as the variable transduction efficiency. Therefore, it is of interest to use a more reliable model to overexpress ELP3 to overcome this limitation. Addictionally, viral transduction was performed in early stages of mice life, what would not be feasable to mimic in humans, has the onset is later in their adulthood life. The use of trangenic mice where time and tissue-specificity of overexpression of the transgene can be controled allows us to bypass the limitation of the viral delivery method.

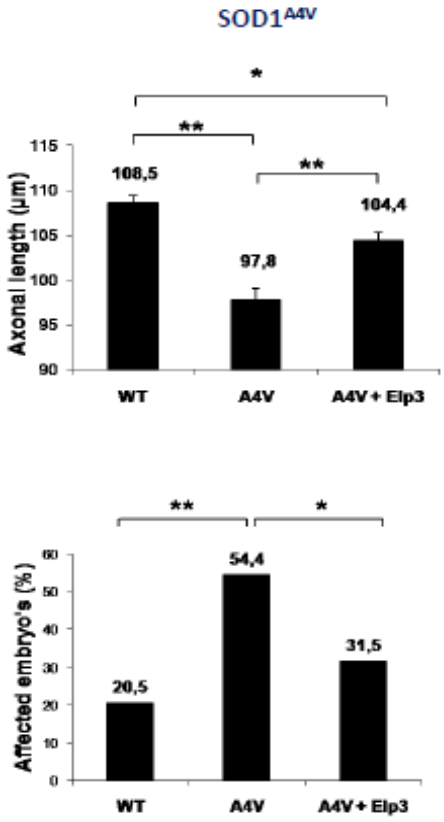

Figure 5. **Elp3 overexpression rescues SOD1A4V phenotype in the Zebrafish.**

To assess the neuronal contribution on the protective role of ELP3 is essential to understand the biological role of this protein. On one hand is of interest to evaluate whether modulation (over and underexpression) of ELP3 affects the progressive motor neuron degeneration present in ALS. On the other hand, since this has not been studied yet, it is also important to identify what are the molecular mechanisms underlying ELP3 protective function, and discover up- and downstream effectors that can be respectively controlling or be controlled by ELP3. Meanwhile, these molecules could be of interest from a therapeutic perspective.

ALS pathology is most certainly a multi-factorial disease. It is known that genetic factors play a role in the pathogenesis of ALS, either as susceptibility genes or modifying factors[2]. Collecting all this data regarding ELP3 function and its correlation with ALS, ELP3 protein seems to be an interesting and promising modifier factor to ALS.

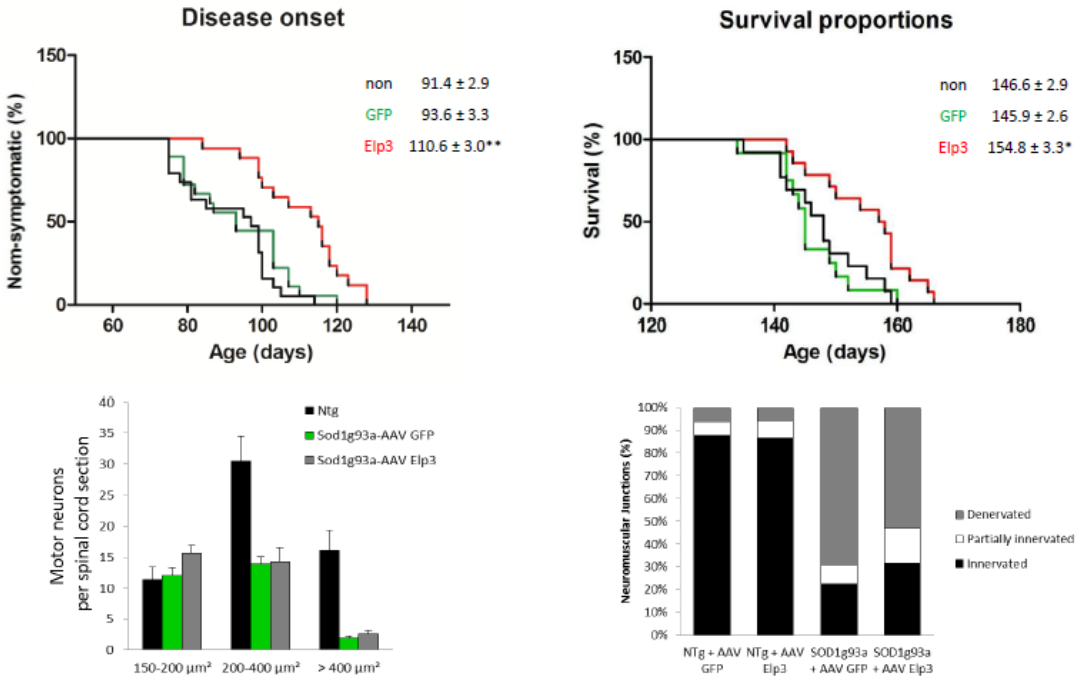

Figure 6. **ELP3 overexpression, by intrathecal delivery of AAV9-ELP3 viral particles, delays disease onset and prolongs survival of SOD1G93A mice.**

1.8. Aims of the study

Considering the eminent evidences that Elp3 is involved in modulation of ALS pathogenesis, this thesis focused on two main research line topics, in which the main goal was to study the role that ELP3 plays as a modifier for ALS. On one hand, to study the effects of Elp3 modulation in different ALS models and, on the other hand, the molecular mechanisms that underlay ELP3 neuromodulator function.

The first objective was to test whether the protective effect of ELP3 overexpression observed previously remain in an up to date and more reliable ALS models. For this purpose two ALS models were used, the C9orf72 HNR zebrafish model and the SOD1G93A transgenic mice overexpressing ELP3 time and tissue-specific,.

The second aim of this master thesis was to identify the molecular mechanism behind ELP3 protective role in ALS. Elongator has been implicated to modify tRNAs at the wobble position, in the yeast. Therefore the aim was to knock down ELP3 expression in zebrafish model and address if overexpression of the specific tRNAs could rescue the motor axonopathy induced by ELP3 deletion.

2. Materials & methods

2.1. Mouse Models

2.1.1. Ethics statement

The principles of Laboratory Animal care by the National Institutes of Health (NIH publication no. 86-23, revised 1996) was taken into account during all animal research regarding proper animal housing, care and experimental procedures. The research was approved by the ethical committee of "Katholieke Universiteit Leuven", Belgium.

2.1.2. Mice lines

SOD^{WT} mice is a mutant strain that carries the normal allele of human SOD1 gene. This transgenic is useful as a control for the *SOD1^{G93A}* mice (B6SJL-Tg(SOD1*G93A)1Gur/J) strain.

SOD1^{G93A} mice (B6SJL-Tg(SOD1*G93A)1Gur/J) was purchased from The Jackson Laboratory. These transgenic strain express a G93A mutant form of human *SOD1* in which glycine is substituted to alanine at codon 93 of the human *SOD1* gene. SOD1^{G93A} mice mimics the phenotype expressed by amyotrophic lateral sclerosis (ALS) patients due to substantial loss of motor neurons at the spinal cord. Pathologic features arise approximately at the age of 60 days, so called as the pre-symptomatic stage, when microgliosis and, later around day 80 of age, astrocytosis emerge. The symptomatic stage starts 90 days after birth, displaying initially extensive tremor and weakness of the hind limb muscles, following severe atrophy and progressive paralysis of the hind limb, so called as a post-symptomatic stage which occurs around 140 days of age. Consequently after 60 days of the disease onset mice start to show progressive disability of gait, eating and drinking what leads to death around day 150[37,40]. This end-stage is determined by the inability to turn to their normal posture in a period of 10 seconds when laying on their back.

Elp3 flox/flox mice were purchased from OZgene Company, Australia. The human Elp3 gene, containing a FLAG tag in the C-terminus, is inserted in the ROSA 26 locus and it is preceded by a STOP cassette flanked by two loxP sites (Figure 7). In the presence of the Cre recombinase, the loxP sites are catalyzed, resulting in the excision (or "flox") of the STOP cassette which consequently allows the expression of the huElp3 (Figure 8).

The CAGG-CreER and the Thy1-CreER mice were purchased from The Jackson Laboratory. The CAGG-CreER mice express the Cre recombinase under the control of the first

exon and the first intron of chicken beta-actin gene (that acts as ubiquitous promoter). The Thy1-CreER mice express Cre recombinase specifically in neurons, under the control of the Thy1 promoter. In both mice, the Cre recombinase expression is achieved after tamoxifen (Sigma, St Louis, USA) administration. The tamoxifen (40 mg/ml in sunflower oil,) is administered at 4mg/day during 4 consecutive days by oral gavage. Tamoxifen binds to the mutant form of the human estrogen receptor (ER^T) which is fused with the Cre recombinase. This mutation at the ligand-binding domain of ER (Gly 521→Arg,G521R) reduces the affinity of endogenous estrogen (e.g. estradiol) whereas it increases for synthetic ligands as tamoxifen[89]. Binding of tamoxifen to the chimeric protein Cre-ER^T is required, once it permits the translocation of the Cre enzyme into the nucleus, where it will excise the loxP sites (Figure 8). This biotechnical tool allows us to choose the day of induction of Cre mediated recombination[90]. This biotechnical tool allows us to choose the day of induction of Cre mediated recombination.

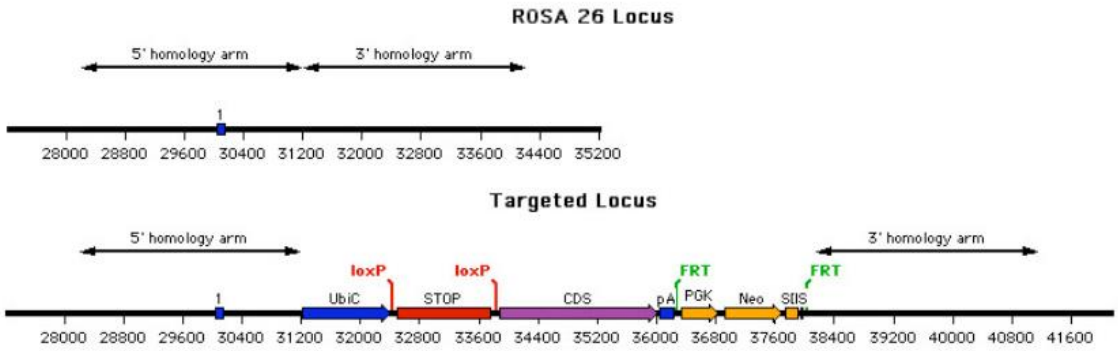

Figure 7. **Elp3 $^{flox/flox}$ construct. This loxP-flanked STOP cassette was inserted into the ROSA26 locus. Under the control of the human Ubiquitin C promoter (UbiC), the target construct, contains signals designed to prevent transcription of the gene of interest (STOP cassette), which is placed between the promoter and the coding sequence (CDS), the last one containing the human Elp3 gene. The STOP cassette can be removed using Cre recombinase by excision at the loxP sites that confines it. (Schematic construct design provided by OZgene Company).**

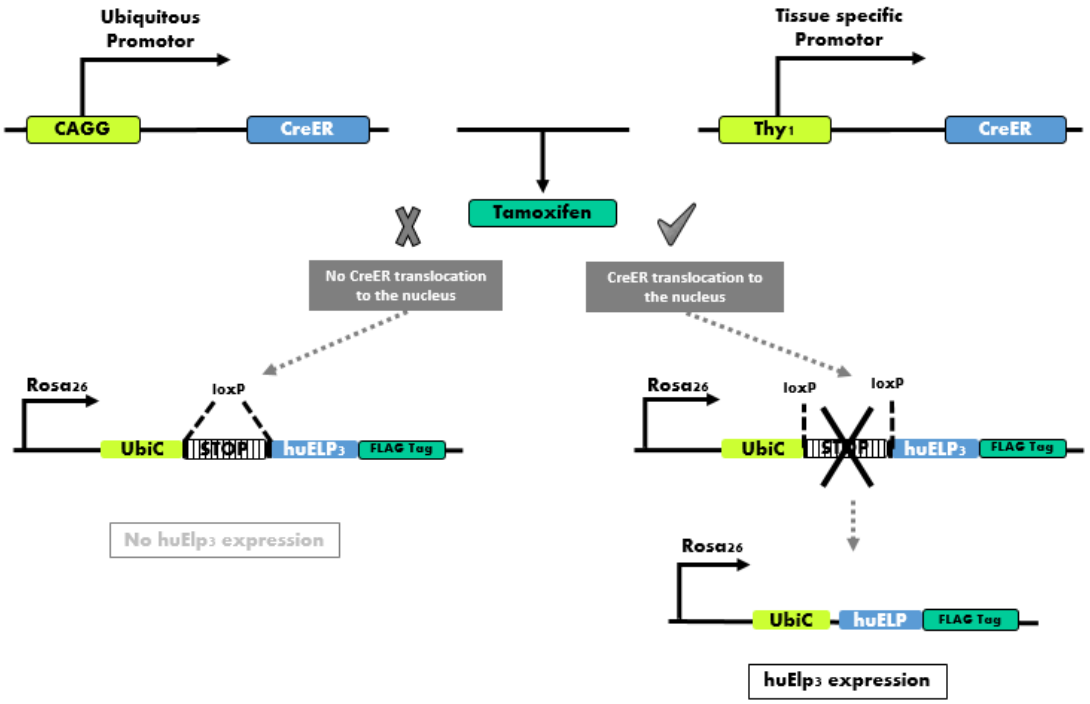

Figure 8. **CreER activation and Tamoxifen dependence. CreEsr is expressed in all cell types when under the control of an ubiquitous promoter like CAGG or only in a certain cell type when under the control of a tissue specific promoter like Thy1. In the absence of Tamoxifen CreEsr does not have access to the nucleus, this way gene excision will not occur (left). In the presence of Tamoxifen CreEsr is able to get into the nucleus where it will induce gene expression as the Stop cassette is excised (right).**

2.1.3. Crossbreeding

ELP3 $^{flox/flox}$/Thy1/SOD1 ^{G93A} and ELP3 $^{flox/flox}$/CAGG/SOD1 ^{G93A}

The crossbreeding was performed with the previous described mice lines and was accomplished already before and during the master thesis period.

To obtain the triple transgenic mice overexpressing huElp3 gene two crossbreed generations were performed. First Elp3$^{flox/flox}$ mice were crossbred with Thy1-CreER mice and simultaneously Elp3$^{flox/flox}$ mice were crossbred with the SOD1^{G93A} mice. Secondly Elp3$^{flox/flox}$/Thy1$^{+/-}$ female mice were crossbreed with the Elp3$^{flox/flox}$/SOD1 $^{G93A\ +/-}$ male mice (as female SOD1 ^{G93A} mice are infertile).

Tamoxifen was administered to Elp3$^{flox/flox}$/Thy1$^{+/-}$/SOD1 ^{G93A} triple transgenic mice and Elp3$^{flox/flox}$/SOD1 ^{G93A} double transgenic mice (lacking the Thy1-CreER gene) 60 days after birth. To evaluate the expression of the human ELP3, the double transgenic mice Elp3$^{flox/flox}$/Thy1$^{+/-}$ were used.

The same strategy was used to obtain the ELP3$^{flox/flox}$/CAGG/SOD1^{G93A} mice.

2.1.4. Mouse genotyping

DNA isolation

Genomic DNA was isolated from 3-4 weeks mice tail tissue (0.5 cm) by incubation with lysis/ alkaline reagent (25 mM NaOH, 0.2 mM EDTA, pH 12.0) at 95°C for one hour. Then a neutralization buffer (40 mM Tris-HCl, pH 6.0-7.0) was added to stop reaction.

Polymerase Chain Reaction (PCR)

Genotyping proceeded via PCR was accomplished in 15 µL reactions containing 2x Dream Taq Green PCR Master Mix (Thermo Fisher Scientific, Reskilde, Denmark) (supplied in 2X DreamTaq Green buffer, dATP, dCTP, dGTP and dTTP, 0.4 mM each, and 4 mM MgCl2), 0.67 µM sense primer, 0.67 µM antisense primer and 2 µL of extracted genomic DNA. Different screenings were necessary to genotype and identify the double and triple transgenic mice. The different amplifications (Applied Biosystems 2720 Thermal Cycler, Foster City, CA, USA) were performed using the following cycling conditions: first an initial denaturation at 94 °C for 5 minutes; then cycle of denaturation (at 94 °C for 30 seconds), annealing and elongation (details on table 2); and lastly a final extension step at 72 °C for 7 minutes. The sequencse of the forward (Fw) and reverse (Rv) primers used are shown in table 3. PCR products were run on a 2 % agarose gel at 126 mV in TBE buffer (Lonza Braine SA, Braine-l'Alleud, Belgium) containing 0.89 M Tris-borate, 0.02 M EDTA (disodium salt), pH 8.3. Bands were compared to Gene Ruler Ladder Mix (Thermo Fisher Scientific, Reskilde, Denmark) and visualized using GelGreen™ (Biotium Inc., Hayward, USA) gel staining and the BioDoc-It imaging system (UVP, Upland, CA).

Table 2. **Denaturation cycles conditions for each PCR screening**

	SOD1 ^{G93A}	**Cre-CAGG**	**Cre-Thy1**	**Elp3$^{f/f}$**	**ROSA-UbiC Elp3 KI**	**ROSA elp3 KI**
Denaturation Cycles	29	35	32	32	32	32
Annealing	55°C/25s	51.7°C/1min	72°C/30s	55.0°C/30s	56°C/45s	56°C/45s
Elongation	72°C/5min	72°C/2min	72°C/7min	72°C/1min	72°C/1min	72°C/1min

Table 2. **Fw & Rv primers used in each PCR screening**

	Forward primer	Reverse primer
SOD1 ^{G93A}	5' CTA GGC CAC AGA ATT GAA AGA TCT 3' 5' CAT CAG CCC TAA TCC ATC TGA 3'	5' GTA GGT GGA AAT TCT AGC ATC ATC C 3' 5' CGC GAC TAA CAA TCA AAG TGA 3'
Cre_CAGG	5'-GCG GTC TGG CAG TAA AAA TAT C-3'	5'-GTG AAA CAG CAT TGC TGT CAC TT-3'
Cre_Thy1	5'-TCT GAG TGG CAA AGG ACC TTA GG-3'	5'-CGC TGA ACT TGT GGC CGT TTA CG-3'
Elp3$^{f/f}$	5'-TAC CTT TCT GGG AGT TCT CTG C-3'	5'-AAC CCC AGA TGA CTA CCT ATC C-3'
ROSA-UbiC Elp3 KI	5'-TAT CAG TAA GGG AGC TGC AGTG-3'	5'-CTG TGA TCG TCA CTT GGT GAG -3'
ROSA elp3 KI	5'-TAC CTT TCT GGG AGT TCT GC-3'	5'-GGA TAG GTA GTC ATC TGG GGT T-3'

2.1.5. Assessment of huElp3 overexpression

Quantitative Real-Time PCR analysis

After tamoxifen administration, mice were anesthetized with 10 % Nembutal (Ceva chemicals, Hornsby, NSW, Australia) and transcardially perfused with 1X PBS (Sigma-Aldrich, St. Louis, USA). Brain and cerebellum were dissected and collected in lysis matrix D tubes (MP Biomedicals, Brussels, Belgium) for posterior homogenization in the MagNA lyser oscillator (Roche, Mannheim, Germany) for three times at 6,500 rpm for 30 seconds. Samples were immediately snap frozen in liquid nitrogen (N_2) to prevent RNase activity and stored at -80 °C until further use. Total RNA was extracted using TriPure (Roche, Basel, Switserland) and isopropanol purification. RNA concentrations were determined by a NanoDrop ND-1000 spectrophotometer (NanoDrop Technologies, DE, USA). Complementary DNA (cDNA) was synthesized from 1 µg total RNA using the Superscript™ III First-Strand Synthesis Mastermix kit for RT-PCR (Invitrogen, Carlsbad, CA). Residual RNA was removed upon RNaseH treatment for 20 minutes at 37 °C. Quantitative Real-Time PCR reactions were performed on 5 µl cDNA (10ng/µl) using TaqMan Universal PCR master mix (Invitrogen, Carlsbad, CA) and following commercially available TaqMan gene expression assays (IDT, Coralville, Iowa, USA): Mm00804536_m1 ELP3 (Mouse endogenous Elp3), Hs00216429_m1 ELP3 (Human Elp3) and 6892429 (Polr2a – housekeeping gene). Samples were run in triplicate in a 96-well plate and thermal cycling was performed on a StepOne-Plus Real-Time PCR system (Applied Biosystems, Foster city, CA, USA) using a rapid (~40 minutes) amplification protocol. The resulting amplification curves were further analyzed by the $\Delta\Delta C_t$ method. Briefly, the number of cycles

at which the fluorescence reaches a fixed threshold (C_t) is the number of PCR cycles required for the probe fluorescence signal to exceed background level. The difference between the C_t of the target gene and the C_t of the best fitting endogenous reference gene also cold as house-keeping gene, is being referred to as ΔC_t. Polr2a gene was already identified as the best fitting reference by previous analyses. To obtain the $\Delta\Delta C_t$, ΔC_t of a control sample - calibrator sample is subtracted from the ΔC_t of the other samples. Then the $2^{-\Delta\Delta Ct}$ formula was used to calculate relative msELP3 and huEpl3 expression levels. Results were presented with the respective standard deviation.

2.1.6. Motor performance evaluation

Rotarot performance

Exercise capacity and motor coordination was assessed using a rotarod treadmill (UGO Basile, VA, Italy). Motor performance was measured based on the time each mouse remained on the rotating rod before falling, during a maximum period of 3 minutes (Figure 9.a). For this test a fixed rotarot program was used, with a rotational speed of 16 rpm. To each mouse three attempts were given. A period of training of one week was given to the mice before tamoxifen administration (60 days of age), this period was crucial for the mice to get familiar with the motorized rod and to supervised baseline motor performance. After Tamoxifen administration the mice were continually tested twice a week till they were sacrificed. The data shown are the averages of all three trials per session ± SEM.

Hanging wire test

The hanging wire test was used to assess hind- and forelimb muscular strength. This test was done before and after Tamoxifen administration (60 days of age) and continued until mice were sacrificed. In this test the mouse was placed on the grid of a conventional housing cage which afterwards was gently turned upside down (Figure 9.b). To avoid injuries the inverted grid was held approximately 60 cm above the soft cage bedding. The time the mice were able to hold on the grid till the moment they fell was recorded in a maximum period of 60 seconds. The mouse that fell off instantaneously were scored with zero seconds. The test was performed with a minimal interval of two days between the test sessions and executed twice a week. Statistical analysis was done using a one-way ANOVA ($p < 0.05$) and Tukey's post-hoc test. Data are presented as mean ± SEM.

Weight/Survival

Weight and survival were also recorded in all transgenic and control mice. Results were presented with standard deviation at each time-point.

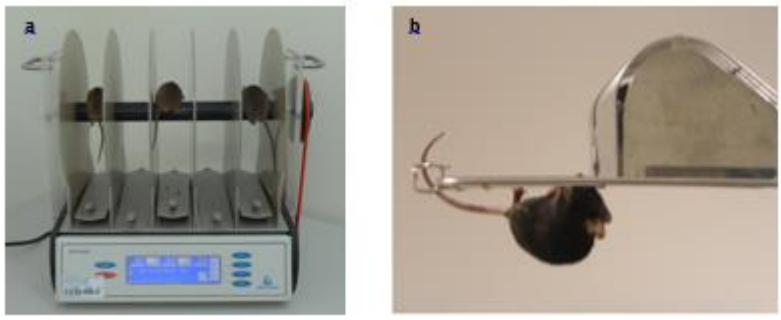

Figure 9**. Motor neuron performance tests. (A) Rotarot performance assessment. (B) Hanging wire test.**

2.1.7. Muscle innervation assessment

Neuromuscular junctions staining

Dissection of the gastrocnemius muscle was performed in the *ELP3* $^{flox/flox}$*/Thy1/SOD1* ^{G93A} and *ELP3* $^{flox/flox}$*/CAGG/SOD1* ^{G93A} mice when anesthetized with 10 % Nembutal (Ceva chemicals, Hornsby, NSW, Australia). Samples (n=2 per genotype) were frozen immediately in isopentane by immersion in liquid nitrogen. Longitudinal sections (20 µm thick) were done once the muscles were already embedding in Tissue-Tek O.C.T compound (Sakura, Antwerp, Belgium). Sections were washed twice with 1X PBS (Sigma-Aldrich, St. Louis, USA) for 5 minutes and blocked with 5 % normal donkey serum (Sigma- Aldrich, St. Louis, USA) in PBST for 1 hour at room temperature. To stain for neuromuscular junctions first the slices were incubated overnight at 4°C with Neurofilament-L (C28E10) Alexa-488-conjugated (1/500, Cell Signaling Technologies, Danvers, MA, USA, #80245) antibody diluted in PBST. In the next day slices were washed four times with PBST followed by incubation for one hour with α - bungarotoxin (B35451) Alexa-555-conjugated (1/5,000, Invitrogen, Carlsbad, CA, B35451). The slices were washed twice with PBST for 5 minutes and mounted with DAPI-containing Vectashield (Vectorlabs Inc., Burlinglame, CA). Zeiss Axio Imager M1 microscope (Carl Zeiss, Jena, Germany) was used to visualize the fluorescent stains, through a monochrome AxioCam Mrm camera.

Neuromuscular junctions counting

In a minimum of 4 gastrocnemius sections from 130 days old mice (n=2 per genotype) a total of 100 neuromuscular junctions was counted. Neuromuscular junctions innervation extent was determined by the overlap of NF-200 (green) and α-bungarotoxin (red). This way, denervated junctions were identified when no overlap of NF-200 and α-bungarotoxin was observed and innervated when there was an overlap of NF-200 branches and α-bungarotoxin. Statistical analysis was performed using an unpaired T-test ($p < 0.05$). Data are presented as mean ± SEM.

2.2. Zebrafish models (Danio rerio)

2.2.1. Ethics statement

Adult and larval zebrafish (Danio rerio) were maintained at the VIB fish facility (Flanders Institute for Biotechnology, Leuven). All fish facility and breeding were performed according to the National and European Guidelines for Animal Welfare. Experiments were performed on wild-type embryos from WIK strain. All procedures were approved by the ethical committee of "Katholieke Universiteit Leuven", Belgium.

2.2.2. Preparation of RNA samples

Plasmids

The pCMV6-Entry vector (Origene, Rockville, USA) (Figure 9) was used to subclone the C9orf72 66x(G4C2) repeat expansion and also the tRNAs (Lysine, glutamic acid and methionine). This plasmid contains a kanamycin resistance gene for bacterial selection. The T7 promoter, for RNA in vitro transcription, is located upstream the ORF, for the C9orf72 plasmid, or immediately behind the sequence coding for the tRNAs.

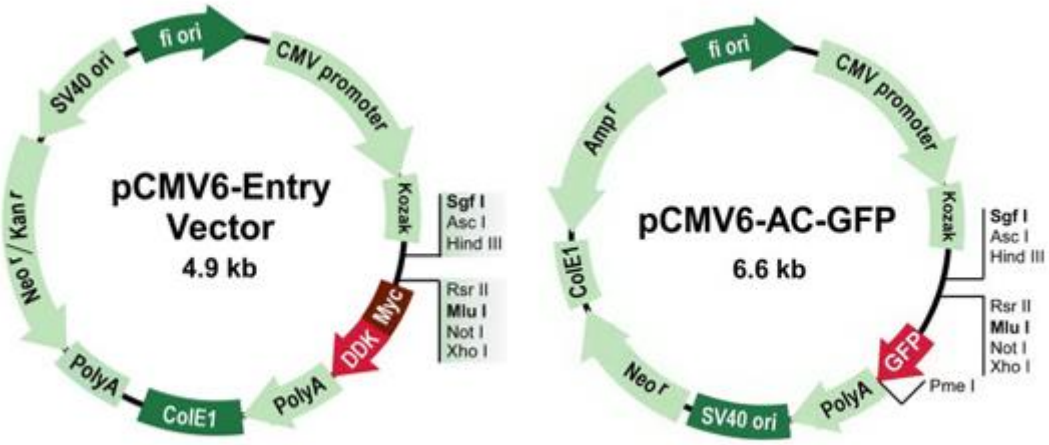

Figure 10. **The Vector Maps of pCMV6-Entry and pCMV6-AC-GFP**

Transformation

Heat-shock transformation procedure was used to introduce our DNA of interest in competent cells (Mix 1µl of DNA (plasmid) into 75µL of competent cells). After 30min on ice the mix was placed for 90 seconds at 42°C and again 2 minutes on ice. Next step was to grow the bacteria in 1mL LB media (without antibiotic) at 37°C in a shaking incubator for 60 minutes. Then transformations were plated onto a 10cm LB agar plate containing the appropriate antibiotic and incubated overnight at 37°C.

Maxi culture - Bacteria growth

Bacterial colonies were separately collected into aliquots of 3mL of LB broth antibiotic and incubated at 37°C shaker overnight (16h). Then tubes content were replaced into 200mL solution of LB broth with the respective antibiotic and placed again at 37°C shaker overnight.

Maxiprep

For maxiprep the PureLink® HiPme Plasmid Filter DNA Purification Kits (Invitrogen) was used. First step provided plasmid DNA isolation. A lysis Buffer (L7) was used, then the lysate was precipitated with the precipitation Buffer (N3). The resulting solution was introduced into a filtration cartridge that is integrated into the DNA-binding column. This way the plasmic DNA got stucked directly in the column membrane. Then columns were washed from impurities and the ultrapure plasmid DNA was then eluted with a high-salt buffer (Elution Buffer (E4)). The

DNA was then desalted and concentrated with an isopropanol precipitation step, then collected by centrifugation and resuspended in 250 µl Nuclease-free Water and restored at -80°C. DNA was quantified by a NanoDrop ND-1000 spectrophotometer (NanoDrop Technologies, DE, USA).

Confirmation of the C9orf72 GGGGCC x66 repeat size by restriction

To make sure that transformation procedure did not interfere with the size repeat restriction analyses were performed. For that a 10µl solution containing 2µl of DNA sample, 2 µl Eco RI and 10x buffer were placed at 37°C for 2 hours. Restriction products were run on a 2 % agarose gel at 126 mV in TBE buffer (Lonza Braine SA, Braine-l'Alleud, Belgium) containing 0.89 M Tris-borate, 0.02 M EDTA (disodium salt), pH 8.3. Bands were compared to Gene Ruler Ladder Mix (Thermo Fisher Scientific, Reskilde, Denmark) and visualized using GelGreen™ (Biotium Inc., Hayward, USA) gel staining and the BioDoc-It imaging system (UVP, Upland, CA).

RNA transcription and purification

The DNA used in the tRNAs transcription was obtained from a PCR product (figure 11). Briefly, the PCR was accomplished in 25 µL reactions containing 10 µM forward primer, 10 µM reverse primer and 1 µL of transformed plasmid DNA in puReTaq Ready-To-Go PCR Beads, containing stabilizers, BSA, dATP, dCTP, dGTP, dTTP, ~2.5 units of puReTaq DNA polymerase and reaction buffer (GE Healthcare Illustra™, Buckinghamshire, UK). The different amplifications (Applied Biosystems 2720 Thermal Cycler, Foster City, CA, USA) were performed using the following cycling conditions: first an initial denaturation at 94 °C for 5 minutes; followed by 32 denaturation cycles at 94 °C for 30 seconds, annealing at 50 °C for 30 seconds, followed by elongation period at 72 °C for 30 seconds; and lastly a final extension step at 72 °C for 7 minutes. The sequence of the forward (Fw) and reverse (Rv) primers used are shown in table 4. PCR products were run on a 2 % agarose gel at 126 mV in TBE buffer.

The DNA used in the C9orf72 66x(G_4C_2) RNA transcription was previously linearized with XhoI restriction enzyme.

The linear DNA template containing the T7 RNA Polymerase promoter in coherent orientation to the target sequence (C9orf72 GGGGCC x66; tK; tE; tM) was transcribed in vitro overnight at 37°C, using a T7 polymerase kit (mMACHINE® T7 Transcription Kit, Ambio) (figure 11). In 20 µl reactions (4X) containing 10 µl 2X NTP/Cap solution, 2 µl T7 Enzyme Mix, 2 µl 10X Reaction Buffer, 3 µl Nuclease-free Water and 3 µl of DNA sample. The transcribed RNA was

purified using Trizol extraction. First 1 µl of DNAse was added to the transcribed product. Secondly 500 µl Trizol followed by 100 µl Cloroform was added to the samples. 15s shaking and 2 min incubation at room temperature (RT), then samples were centrifuged at 4°C for 15 min at 12.000 rpm. Approximately 400 µl supernatant were collected into an RNAse free tube, where 500 µl of isopropanol was added and followed by an incubation time of 10 min a RT. Then centrifuged at 4 °C for 10 minutes at 12.000 rpm and consequently supernatant was removed. Pellet was washed once with 1 ml of 75% ethanol followed by vortex and centrifuged at 4 °C for 5 minutes at 7.500 rpm. Afterwards, the supernatant was removed and the pellet was dried and dissolved in 25 µl Nuclease-free Water and incubated for 10 min at 60°C. RNA was quantified by a NanoDrop ND-1000 spectrophotometer (NanoDrop Technologies, DE, USA).

Tabela 3. **Fw & Rv primers for PCR reactions for tRNA production**

	Forward primer	Reverse primer
tRNA-Lys(K)	5' GTAAAACGACGGCCAGT 3'	5' TCACTGTAAAGAGGTGTTG 3'
tRNA-Glu(E)	5' GTAAAACGACGGCCAGT 3'	5' TATTCTCGCACGGACTAC 3'
tRNA-Met(M)	5' GTAAAACGACGGCCAGT 3'	5' TAGTACGGGAAGGGTATAAC 3'

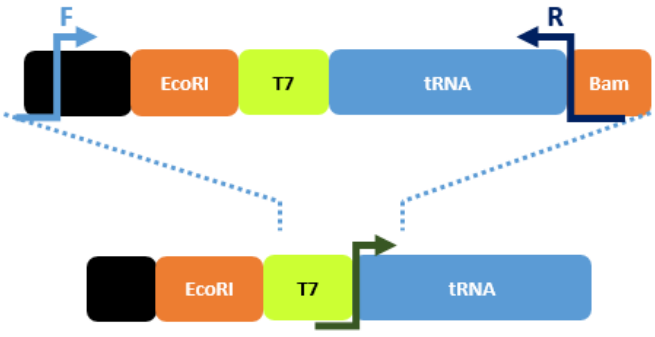

Figure 11. **Scheme of how the target tRNA was extracted from its cloning expression vector (pCMV6-AC-GFP). First a PCR reaction was performed with specific primers, following a transcription reaction using T7 RNA polymerase.**

2.2.3. Microinjection of zebrafish embryos

Injections were performed approximately until minutes pos-fertilization, before embryos reach 4 cell stage blastulae (figure 12.a). An Eppendorf FemtoJet® microinjector pressure system was used to perform the pulse-injections.

HuElp3 and C9orf72 66x(G_4C_2)RNA were injected at 200 ng/µl and 126 ng/ul, respectively. As a control GFP was injected with the highest used injected concentration (200 ng/µl).

Elp3 ATG Morpholino was injected in a concentration of 200 µM. $tRNA^{lys}$, and $tRNA^{gln}$ were injected at 75 ng/µl and 300 ng/µl, respectively. As a control tRNAmet was injected with the same respective concentrations for each $tRNA^{lys}$ or $tRNA^{gln}$ experiment.

2.2.4. Phenotype evaluation

After microinjection, embryos were kept at 28°C and manually dechorionated with two tight forceps at 25hpf. Next, morphological assessment was performed to count and discard death and abnormal embryos from subsequent analysis (Figure 12.b and c).

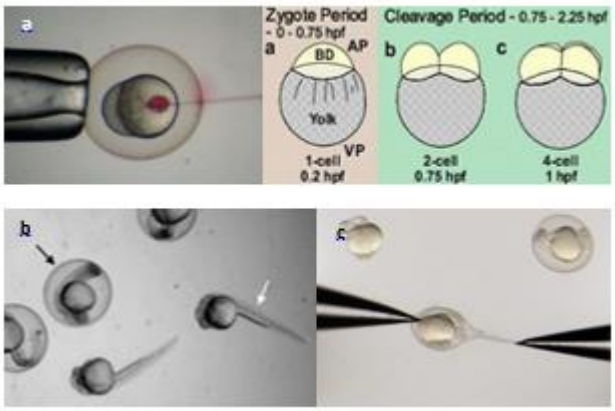

Figure 12. **Zebrafish embryo and its manipulation. (A) Single cell stage of a zebrafish embryo and respective schematic evolution in time post-fertilization form singe to four cell stage. (B) Representation of a normal morphological embryo. (C) Dechorionation process.**

2.2.5. Western blot analysis

Zebrafish were dechorionated and deyolked at 30hpf. Fish were lysated with Radioimmunoprecipitation Assay (RIPA) lysis buffer containing 50 mM Tris-HCl (pH 7.5), 150 mM NaCl, 1 % NP-40, 0.5 % Na-deoxycholic acid, 0.5 % SDS supplemented with EDTA free protease inhibitor cocktail (Complete, Roche, Mannheim, Germany). Lysates were sonicated 10 s, kept on ice for one hour and consequently centrifuged at 4 °C for 20 minutes at 13,200 rpm. Equal amounts of protein were loaded onto a 10 % SDS–polyacrylamide (SDS-PAGE) gel. After electrophoresis, separated proteins were transferred to a polyvinylidene difluoride (PVDF) membrane (Millipore, Overijse, Belgium) by a semi-dry transfer apparatus (TE70XP, Hoefer,

San Fransisco, California) at 180 mA for 1.45 hours. The membrane was then blocked with 5 % skimmed milk in Tris-Buffered Saline containing 10 mM Tris–HCl (pH 7.5), 150 mM NaCl and 1 % Tween-20 (TBS-T) for 1 hour at room temperature. For immunodetection, blots were rinsed with TBS-T and incubated overnight with a primary antibody against ELP3 (rabbit, 1/500; Cell signaling).. After washing the membranes with TBST and incubating them for 1 hour with the appropriate secondary antibody (1:1000; Dako, Glostrup, Denmark), protein bands were visualized using enhanced chemiluminescence (ECL substrate; Pierce, Rockford, USA). Tubulin (mouse, 1/1000, Sigma) was used as a loading control. Blots were scanned using the ImageQuant LAS 4000 Biomolecular Imager (GE Healthcare, Waukesha, WI) and band intensities were quantified using ImageJ software (National Institutes of Health, Bethesda, MD, USA).

2.2.6. Fixation and Immunohistochemistry

To analyze the injected zebrafish embryos, immunohistochemistry was done. First embryos were fixed after 30hpf with 4% paraformaldehyde in phosphate-buffered saline (PBS) during two hours or overnight. Afterwards the samples were washed 3x with PBST (0,1% Triton X-100) at room temperature (RT), followed by an incubation with acetone for 1 hour at -20 degrees. Then fish were incubated in 1% BSA/1%DMSO/ PBS for 1 hour at RT. Incubation with primary antibody SV-2 was performed for 5 hours at RT (1/200 dilution in 1% DMSO/PBS). After being washed for 3x with 1% BSA/1% DMSO/PBS at RT, incubation with secondary antibody AlexaCy555 anti-mouse was done overnight at 4 degrees (1/500 dilution in 1% DMSO/PBS). At the second day the samples were washed 10x with PBST.

2.2.7. Motor neuron axonopathy assessment

The axonal length was measure in the first 5 ventral motor neurons along the yolk sac, starting to count from the 8th neuron, from the exit point of the axon at the ventral part of the spinal cord until its distal tip (figure 13). For the branching 20 ventral motor nerves (10 each site along the yolk sac extension at 30hpf) were analyzed, starting also to count from the 8th neuron. Affected motor neurons were selected when these showed branched axons at or above the ventral edge of the notochord (figure 13). Abnormality was considered when two or more axons for embryo were detected. Whole-amount analyzed embryos were imaged on a

Leica microscope software. Statistical analysis was done using a one-way ANOVA ($p < 0.05$) and Tukey's post-hoc test. Data are presented as mean ± SEM.

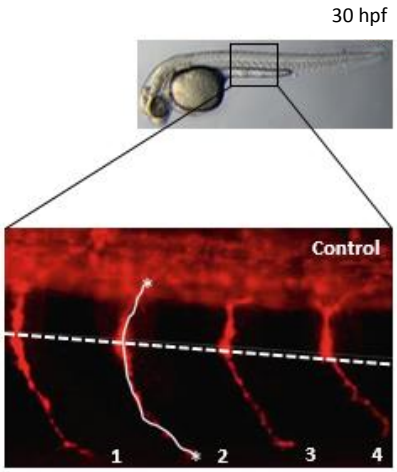

Figure 13. **Motor neuron axonopathy evaluation. Visualization of the first 4 ventral motor neurons along the yolk sac, starting from the 8th neuron. White continuous line representing the axonal scoring length, and dashed line over the notochord ventral edge, delimitating abnormal branched axons zone.**

3. Results

3.1. Effect of ELP3 overexpression in different ALS models

3.1.1. Effect of human ELP3 overexpression in the C9orf72-repeat expansion zebrafish model

Set up of the C9orf72-repeat expansion zebrafish model

In order to better study the role of ELP3 in ALS, a C9orf72-repeat expansion zebrafish, available in the lab, was used. In this model, RNA containing 66x(G_4C_2) repeats is injected in 1-2 cell stage zebrafish, inducing motor axonopathy characterized by reduced axonal length and increased abnormal branching (Figure 14.b). Before injection, the size of the transcribed RNA 66x(G_4C_2) repeat (400bp) was confirmed (figure 14.a). To identify the highest non-toxic concentration of 66x(G_4C_2) RNA that could induce the axonopathy, we performed a toxicity screen. We injected different concentrations of RNA and scored the branching and the length of motor axons and also the viability of the zebrafish. We observed that 126ng/µl of 66x(G_4C_2) RNA was the highest concentration that could induce axonopathy under the pre-defined toxicity threshold (maximum of 35% dead or abnormally developed zebrafish 30hpf) (Figure 14.c, 14.d and 14.e). Of note, this axonopathy is similar to the one observed in the mutant SOD1 zebrafish model[91].

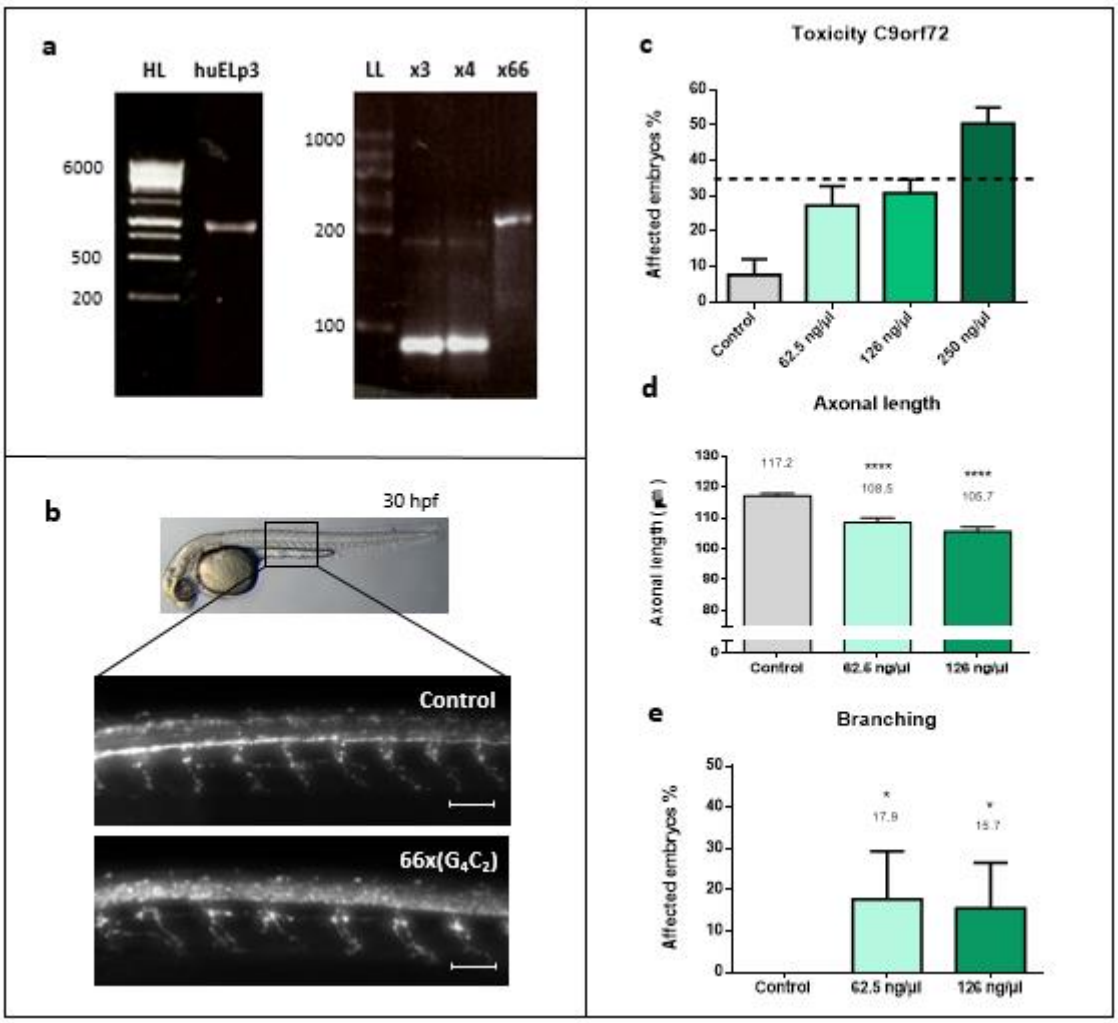

Figure 14. **Toxicity screen for C9orf72 66x(G_4C_2). (A) RNA gel of huELP3 and 66x(G_4C_2) with the respective high (HL) and low (LL) range RNA ladders. (B) Representative images of control and 66x(G_4C_2) RNA injected zebrafish, 30 hpf. Scale bar 50 µm. (C) 126 ng/µl dose identified as the highest non-toxic dose, with more than 65% of viable embryos. (D and E) Effect of 66x(G_4C_2) RNA injection in the axonal length (D) and axonal branching (E). Results show SEM for the axonal length (****P < 0.0001) and mean with 95% CI for the branching (*P = 0.0133).**

Co-injection of human ELP3 and C9orf72 66x(G_4C_2) RNA in the zebrafish embryo

ELP3 was identified as a disease modifier in carries of repeat expansions in the C9orf72 gene[19]. Patients expressing ELP3 variant mutation consequently show an early onset and decrease time of survival[63]. Thus, we hypothesized that ELP3 overexpression could have a protective effect. Therefore, we overexpressed human ELP3 RNA in the C9orf72-repeat expansion zebrafish model and evaluated the phenotype.

Our results show that when human ELP3 RNA was co-injected with C9orf72 66x(G_4C_2) RNA, it could partially prevent the phenotype induced by C9orf72 66x(G_4C_2) RNA alone (figure 15.a and 15.b). However, these results were not statistically significant when compared to the C9orf72 66x(G_4C_2) condition. More experiments should be performed to confirm these results.

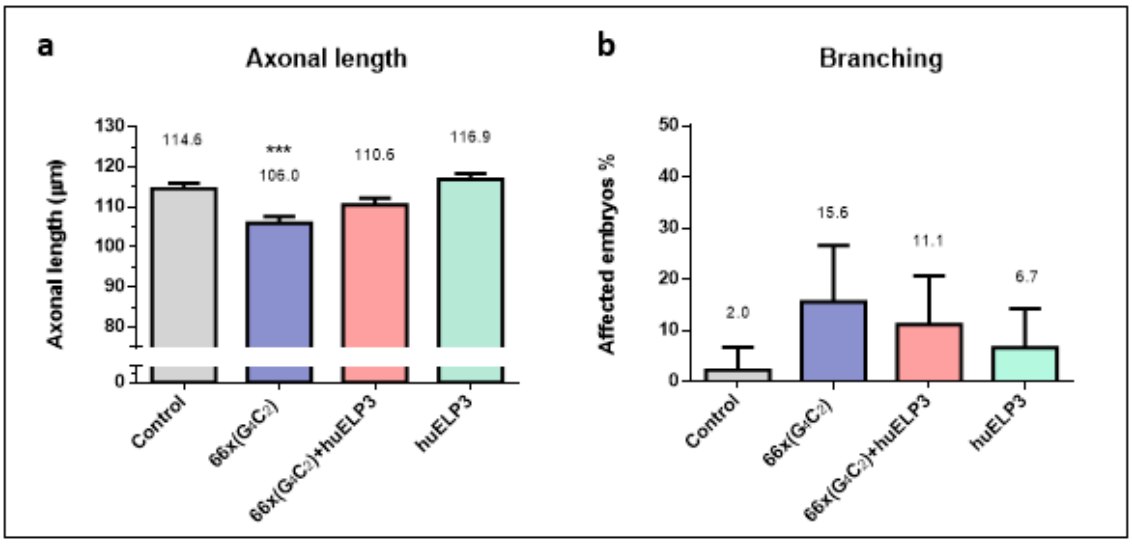

Figure 15. **HuELP3 overexpression partially rescues the C9orf72 66x(G_4C_2) induced axonopathy. (A) There was a partial but not significant increase in axonal length of motor neurons when comparing the co-injection of 66x(G_4C_2) with huELP3 and the respective controls. Results show SEM (***P < 0.05). (B) HuELP3 overexpression resulted in decreased branching of motor axons of the C9orf72 66x(G_4C_2) zebrafish model (n=3). HuELP3 RNA was injected with a concentration of 100 ng/µl.**

3.1.2. Effect of human ELP3 overexpression in the SOD1^{G93A} mouse

Ubiquitous human ELP3 overexpression in the SOD1^{G93A} mouse

Previous research show that ELP3 down regulation induced motor neurodegeneration[1,63]. If ELP3 deletion increases motor neuron vulnerability, then ELP3 over-expression may alleviate this phenotype. Accordingly, it has been shown recently that ELP3 has a neuroprotective effect in the SOD1 zebrafish model and also in the SOD1^{G93A} mouse. The overexpression of human ELP3 in the ALS mouse model was achieved by intrathecal delivery of AAV9. However, the expression levels of the human ELP3 were too variable. To overcome this limitation, the SOD1^{G93A} mouse was crossed with a transgenic mouse overexpressing ELP3 under the control of the inducible and ubiquitous CAGG-CreER promoter. The conditional overexpression of human ELP3 significantly extended the survival of the SOD1^{G93A} mice (163 days vs 153 days). Moreover, the total number of innervated neuromuscular junctions (of the gastrocnemius muscle) was also significantly increased despite the number of motor neurons

in the ventral spinal cord remained unaffected. These data were not obtained during the training period, but it was necessary to describe them to better understand the next section.

Neuronal expression of human ELP3 in the SOD1^{G93A} mouse

Expression of the human ELP3 gene in ELP3$^{flox/flox}$/Thy1-CreER mice

The results obtained with the ELP3$^{flox/flox}$/SOD1/CAGG-CreER mice gave us the insight on the effects of ELP3 overexpression from an ubiquitous perspective, leaving inconclusive notes about the neuronal contribution of ELP3 on its protective role. To overcome this, a transgenic mouse expressing ELP3 under the Thy1 promoter was generated.

To check if the human ELP3 was expressed, we treated adult ELP3$^{flox/flox}$/Cre and ELP3$^{flox/flox}$ mice with tamoxifen and analyzed the mRNA levels in the brain, two weeks after. As expected, the human ELP3 mRNA was detected in the ELP3$^{flox/flox}$/Cre mice and also in the ELP3$^{flox/flox}$. This indicates that there is a "leaky" expression of the transgene, independent of the Cre promoter. Nonetheless, the human ELP3 gene is 3-fold more expressed compared to control mice (Figure 16).

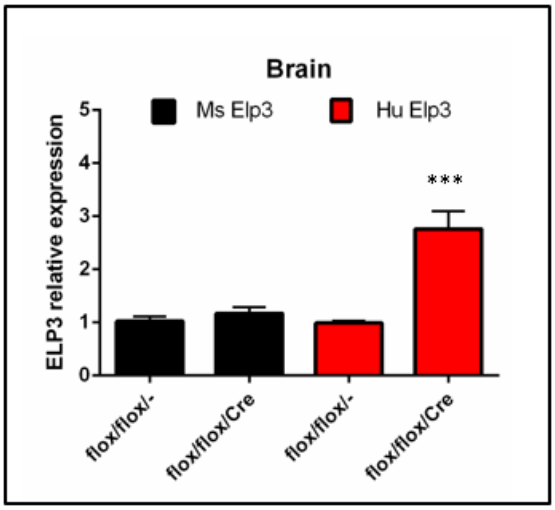

Figure 16. **Thy1Cre-ER recombination efficiency in the brain. Conditional expression of human ELP3. ELP3$^{flox/flox}$ and ELP3$^{flox/flox}$/Thy1-Cre mice were treated with tamoxifen and the expression of human ELP3 and endogenous ELP3 in the brain was evaluated by qPCR. Data represent mean ± SEM, n=3. ***p<0.001.**

Motor performance tests in the ELP3$^{flox/flox}$/SOD1/Thy1-CreER mice

The ELP3$^{flox/flox}$/SOD1/Thy1-CreER mouse strain was, at the time of this master thesis, being expanded. Consequently further crossbreeding's are been performed to complete the preliminary data here presented.

Nonetheless, a small cohort of mice was made available and the motor performance test to determine the disease onset could be performed.

Mice were considered symptomatic when they were unable to complete the rotarod and hanging wire tests. The results show that ELP3$^{flox/flox}$/SOD/Cre and ELP3$^{flox/flox}$/SOD mice suffer a decline in motor ability, while control mice ELP3$^{flox/flox}$ and ELP3$^{flox/flox}$/Cre maintain their performance, in both motor tests (figure 17.a and 17.b). No significant difference was observed at the age of onset of the disease, due to the limited number of mice tested.

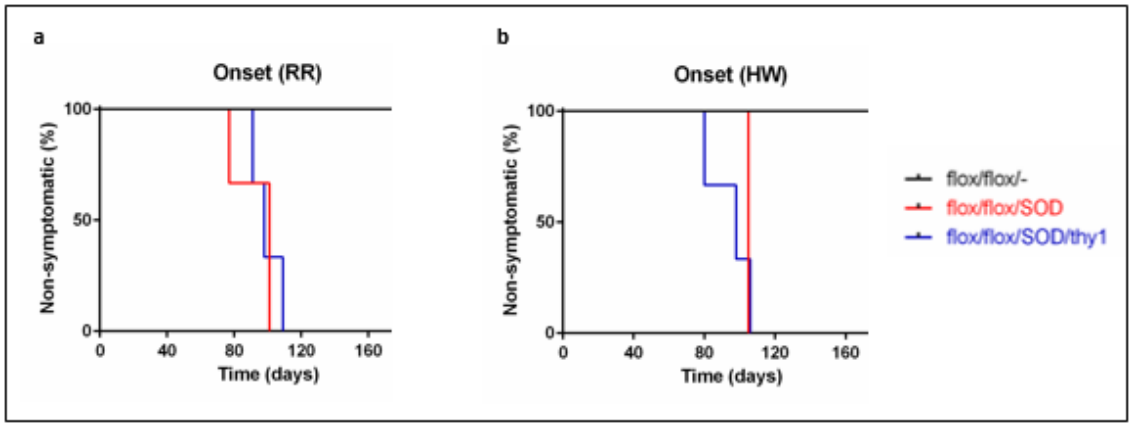

Figure 17. **Motor performance assessment using rotarod (A) and hanging wire tests (B). ELP3$^{flox/flox}$/SOD (n=3) and ELP3$^{flox/flox}$/SOD/Cre (n=4) show a decline motor performance during weekly testing. Control mice, ELP3$^{flox/flox}$ (n=5) and ELP3$^{flox/flox}$/Cre (n=1), show no difference on rotarod and hanging wire tests.**

Evaluation of body weight in the ELP3$^{flox/flox}$/SOD1/Thy1-CreER mice

The body weight is another important parameter that can be evaluated, as a way to monitor the disease progression (and general health condition). The results show a decline in body weight in the SOD1^{G93A} mice, compared to control mice, as a consequence of the progression of the disease. Despite the limited number of mice monitored, the results indicate that overexpression of human ELP3 in the SOD1^{G93A} mice slows the decrease in body weight, compared to SOD1^{G93A} mice not overexpressing human ELP3 (figure 18.a and 18.b).

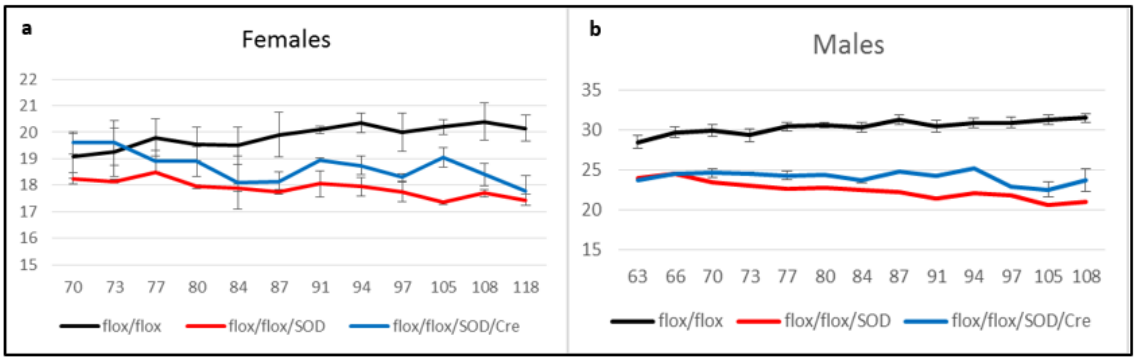

Figure 18. **Body weight curves of female (A) and male (B) mice. ELP3$^{flox/flox}$/SOD: female, n=2; male, n=1. ELP3$^{flox/flox}$/SOD/Cre: female, n=2; male=2. ELP3$^{flox/flox}$: female, n=2; male, n=3.**

3.2. Molecular mechanism underlying ELP3 function

3.2.1. Study of ELP3 protective role: modifications of wobble tRNA

It is of interest to know how ELP3 have the capacity to modulate and affect ALS pathology progression. Exploring the molecular mechanisms behind its neuroprotective properties can unravel possible therapeutic targets. ELP3 was identified in yeast to have an indispensable role in translation via tRNA wobble modifications[6,83-85], as yeast lacking ELP3 are not viable under stress[6]. In particular, ELP3 modifies the wobble uridine of tRNA^{lys}, tRNA^{glu} and tRNA^{gln}. tRNA Lysine (tK) was identified as the one responsible for the rescue of ELP3 deletion phenotype in yeast[6], but tRNA Glutamate (tE), which also undergoes wobble modification by ELP3, did not show to rescue ELP3 deletion in yeast. Thus, we wanted to study if this well characterized process was also at play in vertebrates. We have done this in the zebrafish. We injected an ATG morpholino against ELP3 to reduce its expression and then co-injected it with the known implicated tRNAs, and assessed the axonal length and the axonal branching. As a control, we used the tRNA Methionine (tM), which codes for the initiation codon (AUG) known not to get posttranscriptional wobble modifications.

tRNAs Toxicity Screen

Expected size of tRNAs (80bp) were obtained after transcription with T7 (figure 19.a). First, we needed to address which concentrations of the tRNAs could be injected, without having toxic effects. For that the highest nontoxic concentration was identified using the same assay previously described – toxicity assay, based on affected fish embryos. Our results show that injecting less than 400 ng/µl of tM and tE RNA is not toxic to the fish (figure 19.b and 19.c), while the highest non-toxic concentration for tK was 75 ng/µl RNA (figure 19.d). Concentrations were not toxic when < 35% embryos were affected.

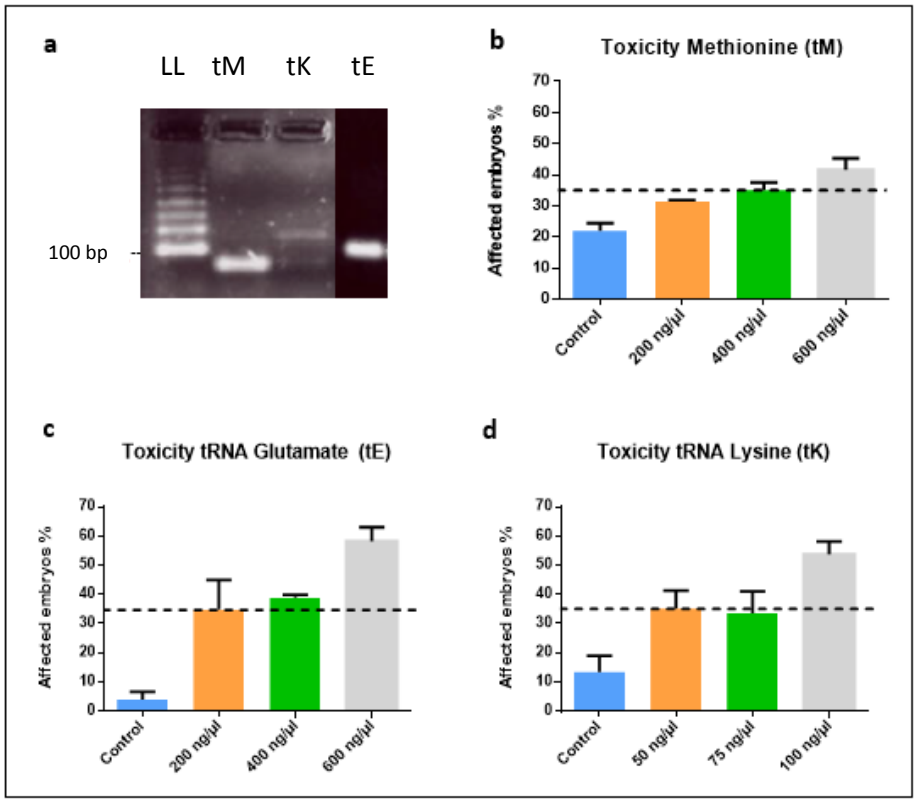

Figure 19. **(A) RNA gel of tRNAs (tM; tK; tE) with the respective low range RNA ladder (LL). (B-D) Toxicity screen for tRNAs. 400 ng/µl, 200 ng/ul and 75 ng/ul dose identified as the highest non-toxic dose, with more than 65% of viable embryos, for $tRNA^{met}$ (B), $tRNA^{glu}$ (C) and $tRNA^{lys}$ (D). Data are shown as a mean of ± SEM (B, n=4; C, n=4; D, n=3)**

Effect of the tRNAs on the phenotype induced by ELP3 know-down in the zebrafish

After assessing the highest non-toxic doses for the tRNAs to be tested, we then confirmed the phenotype induced by the knock-down of the endogenous ELP3 in the zebrafish. Injection of a specific ELP3 ATG morpholino (MO) induces an axonopathy, characterized by reduced axonal length and increased axonal branching (Figure 20.a and 20.b). Western blot analysis shows a decrease of ELP3 protein expression when ELP3 ATG MO was injected (Figure 20.c).

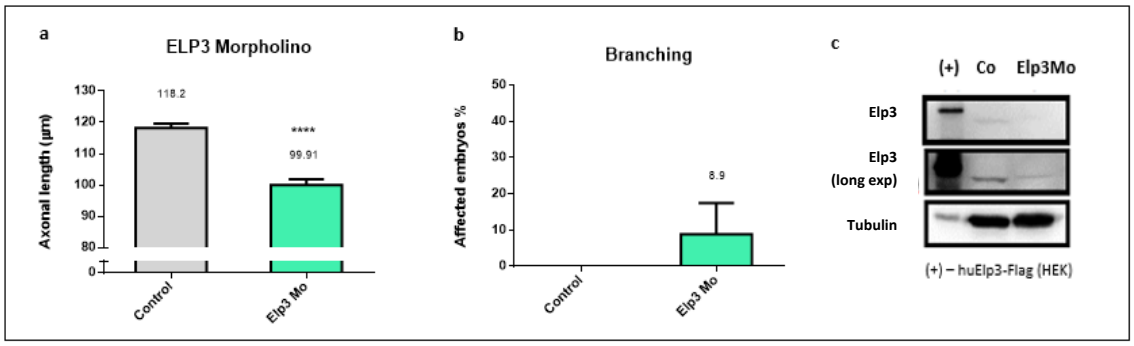

Figure 20. **Axonal length (A), axonal branching (B) and protein expression (C) in zebrafish injected with or without ELP3 ATG MO. In C, Western blot analysis was done using a polyclonal antibody against ELP3. HEK cells transiently transfected with human ELP3 were used as positive control (+).**

Next we evaluated the effect of co-injecting $tRNA^{gln}$ (tE) in the axonopathy induced by ELP3 ATG MO in the zebrafish. No significant differences on the axonal length and axonal branching were observed when compared to the ELP3 ATG MO injected fish (figure 21.a and 21.b, respectively). Co-injection of the $tRNA^{met}$ (tM) did not significantly modify the phenotype induced by ELP3 ATG MO alone (Figure 21.a and 21.b).

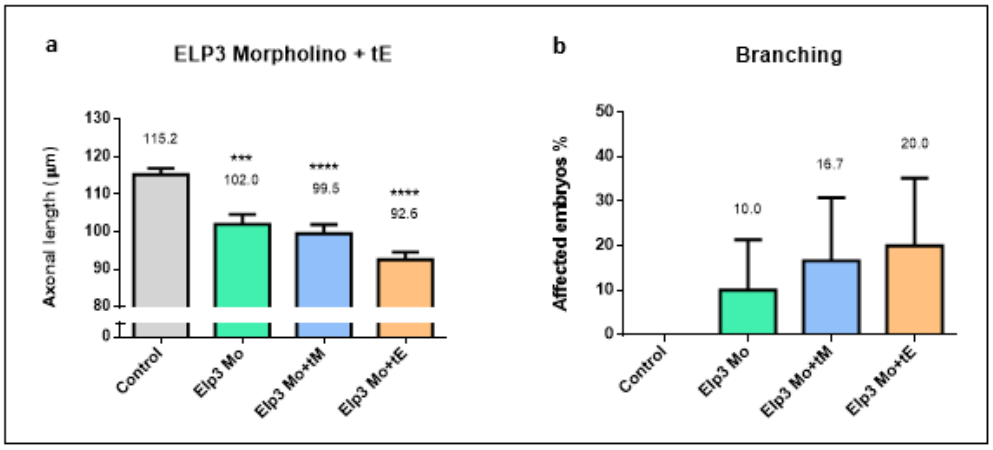

Figura 21. **Figure 20. Axonal length (A) and axonal branching (B) in zebrafish co-injected with ELP3 ATG MO (200 µM) and $tRNA^{gln}$ RNA (300 ng/µl) or $tRNA^{met}$ RNA (300 ng/µl), compared to zebrafish injected with ELP3 ATG MO alone. Results show SEM, ****P < 0.0001, n = 2.**

Finally, we evaluated the effect of co-injecting $tRNA^{lys}$ (tK) in the axonopathy induced by ELP3 ATG MO in the zebrafish. Our results show that $tRNA^{lys}$ partially prevents the increase of axonal branching, unlike $tRNA^{met}$ (Figure 22.b). $tRNA^{lys}$ also prevents, partially, the reduction of the axonal length. Nonetheless, the same result on axonal length was observed when $tRNA^{met}$ was co-injected (Figure 22.a).

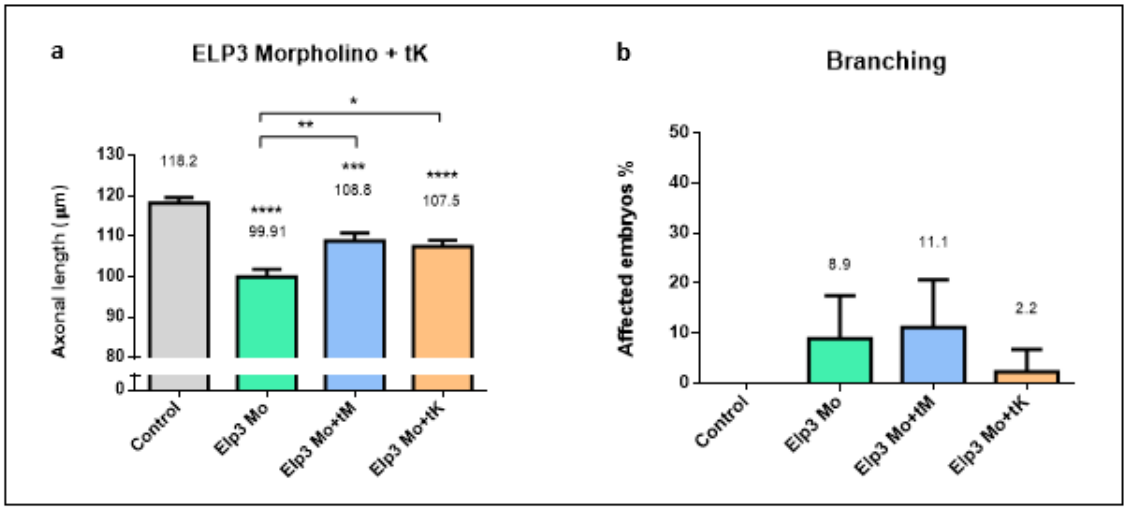

Figura 22. **Axonal length (A) and axonal branching (B) in zebrafish co-injected with ELP3 ATG MO (200 µM) and $tRNA^{lys}$ RNA (75 ng/µl) or $tRNA^{met}$ RNA (75 ng/µl), compared to zebrafish injected with ELP3 ATG MO alone. Results show SEM, ****P < 0.0001, n = 3.**

4. Discussion

It is known that mutations in a heterogeneous set of genes as C9orf72, SOD1, TDP43 or FUS have been identified as the major contributor causes in ALS[2]. Beside the eminent role that these genetic factors play in ALS other modifying factors or susceptibility genes were identified as being part of this pathology[1,92,93]. Nonetheless, ALS seems to be a multifactorial disease[60,94,95], where modifying molecular targets can be worth to explore looking beyond for future promising novel therapies that could control disease progression.

In this context ELP3 was found playing a role in ALS pathology modulation. A genome wide association study performed with sporadic ALS patients revealed the existence of a polymorphisms on the ELP3 gene associated with decrease risk for ALS. This exciting finding was in line with three other experiments in the same study. First, an independent genetic screen in drosophila identified two different loss-of-function mutations on the homologue of ELP3 that leaded to synaptic defects and aberrant axonal outgrowth. Second, a knock-down ELP3 experiment in zebrafish that was able to induce motor axonal abnormalities comparable to those observed in SOD1 and TDP43 mutant zebrafish model. Third, reduced expression levels of ELP3 in the brain of ALS individuals with the at-risk allele was detected[1]. On another study, ELP3 gene was reported as potential protective disease modifier, increasing survival in MND and/or FTD patients carrying the most frequent genetic cause of these diseases, the C9orf72 repeat expansion[63].

The aim of this project was to further investigate the role of ELP3 as a disease modifier. Additional studies from Dr. Robberecht's lab came to support the neuroprotective role of ELP3 in different ALS models. First, they generated a constitutive ELP3 knockout mouse, which they found to be not viable, dying around day 10 in utero, like the ELP1 knockout mouse[96]. In this study ELP1, a component of the elongator complex, was found to be essential during embryonic development, having a crucial role in neuronal development and associated neurogenesis[96]. Moreover, overexpressing ELP3 in SOD1 mutant zebrafish showed to be protective, decreasing its motor axonopathy abnormalities. Finally, they showed that ELP3 overexpression by intrathecal delivery of AAV9-ELP3 viral particles in neonatal $SOD1^{G93A}$ mice was neuroprotective.

Taking all together, these results lead to the hypothesis that low levels of ELP3 may increase motor neurons vulnerability to neurodegeneration, whereas overexpression may be protective. It is known that ELP3 is critical for proper function of RNA-processing pathways,

especially for efficient translation of highly expressed stress-induced mRNAs. Therefore, ELP3 deletion might increase vulnerability of motor neurons in ALS patients by dysregulation of specific mRNAs, while overexpression could alleviate it.

Our hypothesis on ELP3 overexpression protective effect was tested using two different models, the zebrafish and the mouse ALS models.

The zebrafish has a well-characterized spinal motor system, with overall similarity to humans and due to the high conservation of genes implicated in neurodegenerative diseases. Several zebrafish models have been developed for different neurodegenerative diseases such as Huntington's disease, spinomuscular atrophy (SMA) and ALS[97]. Pilot experiments emerged with the mutated SOD1 zebrafish model. Injection of the mutated SOD1 mRNA in zebrafish embryos showed remarkable specific motor neuron axonopathy mimicking the distal axonopathy observed in rodent models of ALS and in ALS patients[91]. The zebrafish model presents several other advantages. It is a vertebrate model of small size associated with the reduced costs of maintenance. Additionally, zebrafish fertilization results in a large sample size of transparent eggs that are rapidly, externally and in synchrony fertilized, in which the first day of development corresponds approximately to the first trimester of the mammalian development[98]. Consequently, the experiments turn to be faster, with the possibility to perform high-throughput drug screens, genetic manipulation by injection of AMO or mRNAs and anatomical and dynamic processes observations through immunofluorescence[98,99].

We investigated the phenotype of the C9orf72 HNR zebrafish model when ELP3 was overexpressed. A partial rescue on the C9orf72-induced axonopathy was observed. This results are similar to the ones found in the mutant SOD1 fish model, obtained previously in the lab. Nonetheless, statistical significance was not achieved for the C9orf72 RNA+huELP3 RNA co-injection condition, both for axonal branching and axonal length. One explanation can be the reduced number of experimental injections performed. Thus, an increased number of experiments are needed to confirm this tendency.

To overcome the limitation of variability in transduction efficiency that comes out with the viral ELP3 overexpression, a transgenic ELP3 KI $SOD1^{G93A}$ mouse ubiquitously and conditionally expressing human ELP3 was also tested. $SOD1^{G93A}$ mice overexpressing ELP3 showed a life span of 163 days, increasing $SOD1^{G93A}$ mice survival in 10 days. This data is in line with the results obtained by the AAV9-mediated expression of ELP3 in the $SOD1^{G93A}$ mice. However, no significant effect was observed on disease onset, compared to the AAV9:ELP3 $SOD1^{G93A}$ mice. A possible explanation for this can be the time when ELP3 overexpression is induced, showing that if ELP3 is increased early in life it might be critical to delay the trigger for neurodegeneration and consequent emerge of first disease symptoms, while conditional

overexpression it in mice with 60 days after birth by tamoxifen delivery, would not have the same preventive effect, once these are already in a primary pathological stage. After phenotype evaluation, quantification of neuromuscular junctions was done to assess evolution of the pathological remarks. A decrease in denervation (and consequent increase in innervation) was found as a consequence of ELP3 overexpression in ELP3 KI SOD1^{G93A} mice. Nonetheless, the quantification of remaining lumbar motor neurons in the ubiquitous ELP3 KI SOD1^{G93A} mouse and respective controls, showed no significant difference. The higher number of innervated NMJs with the same number of lumbar motor neurons, builds the idea of motor unit expansion where the number of muscle fibers per motor neuron increase. This fact leads to the hypothesis that a possible ELP3 function works forward to motor neuron and muscle connection improvement by adaptive and compensatory sprouting from preserve axons.

Pilot reports showed that other cells besides motor neurons have an active influence in axonal sprouting. Stimulating signals for axonal sprouting can indeed be supported by Schwann cells or even by the denervated muscle fibers[100,101]. This way to assess if ELP3 protective role is restricted to neuronal contribution, similar overexpress of ELP3 was done but now under the control of the tissue specific Thy1 promoter, to specifically overexpress ELP3 in neurons only. Thus, we wanted to address if ELP3 overexpression in neurons would mimic the optimistic results obtained in the mice ubiquitously expressing ELP3. So far merely preliminary data was collected, from which we cannot make any conclusion. Consequently, more mice are needed to confirm the exiting observations obtained with the ubiquitous ELP3 KI SOD1^{G93A} mice. However, these findings indicate that ELP3 overexpression improves motor neuron viability and muscle innervation.

The mechanisms mediating this protective role are still to be unfolded. This way as a second aim for this project we wanted to address what were the mechanisms behind the observed protective effects when ELP3 was overexpressed.

ELP3 was found in yeast being a member of the Elongator complex[102]. Crucial roles were associated since then. Transcription elongation promotion by its close connected with RNA polymerase II complex and histones acetylation, modifying DNA chromatin structure and consequent upgrade of gene transcription[67]. More recently similar activity was found in the cytoplasm, more specifically at the synapse, where it acetylates a large cytoskeletal-like protein – Bruchpilot. This process show to be essential for proper synaptic function keeping the structural architecture at the active zones and consequent regulation of neurotransmitters realize[88]. Not less important, ELP3 was showed to be necessary to increase translation efficiency as it is involved in tRNA wobble modification, being required for side chain modifications of uridines at the 34 position[65,69,83,85]. However it is of interest to know whether

ELP3 is mediating directly all of these functions or if it controls only one of them that in turn triggers the different observed effects. It has been already suggested that the main role of ELP3 is its capacity to modify wobble uridines in tRNAs[103]. Nonetheless, recently an interesting article showed that a specific tRNA – $tRNA^{lys}_{UUU}$ (tK), was mediating the rescue of ELP3 deletion in yeast under stress. This is because the modification of this tRNA is essential for efficient translation of highly expressed stress-induced mRNAs of transcription factors, required for proper transcription of important genes under stress conditions[6].

To understand ELP3 protective function obtained in our ALS models, we wondered if in the zebrafish, the well characterized ELP3-related tRNA wobble modifications were also affected as observed in yeast. Thus, we investigated if overexpressing the $tRNA^{lys}$ in zebrafish lacking ELP3 expression could protect from the axonopathy induced by the knock-down of ELP3. We could indeed see a partial rescue in axonal branching when compared to ELP3 MO injected fish. Nonetheless, we also got a partial rescue when injecting $tRNA^{met}$, our negative control. This tRNA is only required for initial translation and was shown not to undergo posttranscriptional wobble modification. A possible explanation for the obtained results can be a difference in the injected ELP3 morpholino concentration between the different conditions.

Our analysis showed to be inconclusive. However reduced number of experiments were behind these results. Therefore to make further conclusions more experiments should be performed.

5. Conclusion & Future Perspectives

In summary, our results suggest that increasing ELP3 is beneficial in several ALS models. In fact, ELP3 overexpression could partial rescue the C9orf72 phenotype in Zebrafish, delay disease onset, extend survival and improve NMJs innervation in the $SOD1^{G93A}$ mice.

To complete this outcomes additional results concerning the ELP3 cellular target still need to be addressed from the in progress Thy1Cre-ER mouse line. Extra experiments must to be conducted for total understanding of ELP3 as an ALS modifier, namely experiments showing the effects of ELP3 reduction. This can be achieved crossing the $SOD1^{G93A}$ mice with a constitutive ELP3 heterozygous knockout mouse. ELP3 can also be deleted in adult mice both ubiquitously and motor neuron specific using the dependent tamoxifen Cre-ER lox system.

On the other hand, the mechanism behind the observed protective role remains to be discovered. Based on our inconclusive results, experiments concerning ELP3-related tRNA wobble modifications in zebrafish still needs to be further investigated.

To overcome these results, some questions need to be answered. First of all, are wobble modified tRNAs carried by ELP3 affected in other organisms then yeast, like vertebrates as fish and mammals? Answering this question is of extremely importance to know if it is worth to proceed the investigation in this direction. A previous study in Familial Dysautonomia (FD), showed that decreased levels of wobble modified tRNAs in brain tissue and fibroblast cells from FD patients were associated with the typical low levels of ELP1 protein[104], a protein known to be part of the Elongator complex. This way it would be interesting to analyze if the ELP3 conditional knockout mice express reduced level of wobble modified tRNAs.

Yet, other ways to gain insight into the molecular mechanisms underlying ELP3 function should not be discarded. Searching for new downstream effector of ELP3 is a possibility. Based on the well characterized ELP3 deletion phenotype in under stress yeast, genome-wide screen assay could be performed to identify candidate proteins and/or genes with the capacity to modify ELP3 lethal phenotype in yeast. Additional proteomic experiments can be done, for instance analysis of brain and spinal cord of ELP3 conditional knock out mice or cell lines, to identify variability of protein expression levels in the absence of ELP3.

In conclusion, ELP3 is indeed an effective modifier for ALS, thus further investigation into the molecular mechanisms underlying ELP3 function, in particular the identification of potential proteins regulated by ELP3 is of great interest from a therapeutic perspective.

Bibliography

1 Simpson, C. L. *et al.* Variants of the elongator protein 3 (ELP3) gene are associated with motor neuron degeneration. *Human molecular genetics* **18**, 472-481, doi:10.1093/hmg/ddn375 (2009).

2 Robberecht, W. & Philips, T. The changing scene of amyotrophic lateral sclerosis. *Nature reviews. Neuroscience* **14**, 248-264, doi:10.1038/nrn3430 (2013).

3 Chen, C., Tuck, S. & Byström, A. S. Defects in tRNA modification associated with neurological and developmental dysfunctions in Caenorhabditis elegans elongator mutants. *PLoS genetics* **5**, doi:10.1371/journal.pgen.1000561 (2009).

4 Bento-Abreu, A., Van Damme, P., Van Den Bosch, L. & Robberecht, W. The neurobiology of amyotrophic lateral sclerosis. *The European journal of neuroscience* **31**, 2247-2265, doi:10.1111/j.1460-9568.2010.07260.x (2010).

5 Nguyen, L., Humbert, S., Saudou, F. & Chariot, A. Elongator - an emerging role in neurological disorders. *Trends in molecular medicine* **16**, 1-6, doi:10.1016/j.molmed.2009.11.002 (2010).

6 Fernández-Vázquez, J. *et al.* Modification of tRNA(Lys) UUU by elongator is essential for efficient translation of stress mRNAs. *PLoS genetics* **9**, doi:10.1371/journal.pgen.1003647 (2013).

7 Boillée, S., Vande Velde, C. & W. Cleveland, D. ALS: A Disease of Motor Neurons and Their Nonneuronal Neighbors. *Neuron* **52**, doi:10.1016/j.neuron.2006.09.018 (2006).

8 D Rothstein, J. Current hypotheses for the underlying biology of amyotrophic lateral sclerosis. *Annals of neurology* **65 Suppl 1**, 9, doi:10.1002/ana.21543 (2009).

9 Gordon, P. H. *et al.* The natural history of primary lateral sclerosis. *Neurology* **66**, 647-653, doi:10.1212/01.wnl.0000200962.94777.71 (2006).

10 Andersen, P. M. & Al-Chalabi, A. Clinical genetics of amyotrophic lateral sclerosis: what do we really know? *Nature reviews. Neurology* **7**, 603-615, doi:10.1038/nrneurol.2011.150 (2011).

11 Li, T. M., Alberman, E. & Swash, M. Comparison of sporadic and familial disease amongst 580 cases of motor neuron disease. *Journal of neurology, neurosurgery, and psychiatry* **51**, 778-784 (1988).

12 Forsberg, K. *et al.* Novel antibodies reveal inclusions containing non-native SOD1 in sporadic ALS patients. *PloS one* **5**, doi:10.1371/journal.pone.0011552 (2010).

13 Bosco, D. A. *et al.* Wild-type and mutant SOD1 share an aberrant conformation and a common pathogenic pathway in ALS. *Nature neuroscience* **13**, 1396-1403, doi:10.1038/nn.2660 (2010).

14 Tikka, T. M. *et al.* Minocycline prevents neurotoxicity induced by cerebrospinal fluid from patients with motor neurone disease. *Brain : a journal of neurology* **125**, 722-731 (2002).

15 Sojka, P., Andersen, P. M. & Forsgren, L. Effects of riluzole on symptom progression in amyotrophic lateral sclerosis. *Lancet* **349**, 176-177 (1997).

16 DeJesus-Hernandez, M. *et al.* Expanded GGGGCC hexanucleotide repeat in noncoding region of C9ORF72 causes chromosome 9p-linked FTD and ALS. *Neuron* **72**, 245-256, doi:10.1016/j.neuron.2011.09.011 (2011).

17 Renton, A. E. *et al.* A hexanucleotide repeat expansion in C9ORF72 is the cause of chromosome 9p21-linked ALS-FTD. *Neuron* **72**, 257-268, doi:10.1016/j.neuron.2011.09.010 (2011).

18 Renton, A. E., Chiò, A. & Traynor, B. J. State of play in amyotrophic lateral sclerosis genetics. *Nature neuroscience* **17**, 17-23, doi:10.1038/nn.3584 (2014).

19 van Blitterswijk, M., DeJesus-Hernandez, M. & Rademakers, R. How do C9ORF72 repeat expansions cause amyotrophic lateral sclerosis and frontotemporal dementia: can we learn from other noncoding repeat expansion disorders? *Current opinion in neurology* **25**, 689-700, doi:10.1097/WCO.0b013e32835a3efb (2012).

20 Rohrer, J. D. *et al.* C9orf72 expansions in frontotemporal dementia and amyotrophic lateral sclerosis. *The Lancet. Neurology* **14**, 291-301, doi:10.1016/S1474-4422(14)70233-9 (2015).

21 Mackenzie, I. R., Frick, P. & Neumann, M. The neuropathology associated with repeat expansions in the C9ORF72 gene. *Acta neuropathologica* **127**, 347-357, doi:10.1007/s00401-013-1232-4 (2014).

22 Cooper-Knock, J. *et al.* Clinico-pathological features in amyotrophic lateral sclerosis with expansions in C9ORF72. *Brain : a journal of neurology* **135**, 751-764, doi:10.1093/brain/awr365 (2012).
23 Al-Sarraj, S. *et al.* p62 positive, TDP-43 negative, neuronal cytoplasmic and intranuclear inclusions in the cerebellum and hippocampus define the pathology of C9orf72-linked FTLD and MND/ALS. *Acta neuropathologica* **122**, 691-702, doi:10.1007/s00401-011-0911-2 (2011).
24 King, A., Maekawa, S., Bodi, I., Troakes, C. & Al-Sarraj, S. Ubiquitinated, p62 immunopositive cerebellar cortical neuronal inclusions are evident across the spectrum of TDP-43 proteinopathies but are only rarely additionally immunopositive for phosphorylation-dependent TDP-43. *Neuropathology : official journal of the Japanese Society of Neuropathology* **31**, 239-249, doi:10.1111/j.1440-1789.2010.01171.x (2011).
25 Cooper-Knock, J., Kirby, J., Highley, R. & Shaw, P. J. The Spectrum of C9orf72-mediated Neurodegeneration and Amyotrophic Lateral Sclerosis. *Neurotherapeutics : the journal of the American Society for Experimental NeuroTherapeutics* **12**, 326-339, doi:10.1007/s13311-015-0342-1 (2015).
26 Waite, A. J. *et al.* Reduced C9orf72 protein levels in frontal cortex of amyotrophic lateral sclerosis and frontotemporal degeneration brain with the C9ORF72 hexanucleotide repeat expansion. *Neurobiology of aging* **35**, 177900000-646832128, doi:10.1016/j.neurobiolaging.2014.01.016 (2014).
27 Cooper-Knock, J. *et al.* C9ORF72 transcription in a frontotemporal dementia case with two expanded alleles. *Neurology* **81**, 1719-1721, doi:10.1212/01.wnl.0000435295.41974.2e (2013).
28 Fratta, P. *et al.* Homozygosity for the C9orf72 GGGGCC repeat expansion in frontotemporal dementia. *Acta neuropathologica* **126**, 401-409, doi:10.1007/s00401-013-1147-0 (2013).
29 Haeusler, A. R. *et al.* C9orf72 nucleotide repeat structures initiate molecular cascades of disease. *Nature* **507**, 195-200, doi:10.1038/nature13124 (2014).
30 Barmada, S. J. Linking RNA dysfunction and neurodegeneration in amyotrophic lateral sclerosis. *Neurotherapeutics : the journal of the American Society for Experimental NeuroTherapeutics* **12**, 340-351, doi:10.1007/s13311-015-0340-3 (2015).
31 Kearse, M. G. & Todd, P. K. Repeat-associated non-AUG translation and its impact in neurodegenerative disease. *Neurotherapeutics : the journal of the American Society for Experimental NeuroTherapeutics* **11**, 721-731, doi:10.1007/s13311-014-0292-z (2014).
32 R. Rosen, D. *et al.* Mutations in Cu/Zn superoxide dismutase gene are associated with familial amyotrophic lateral sclerosis. *Nature* **362**, 59-62, doi:10.1038/362059a0 (1993).
33 Borchelt, D. R. *et al.* Superoxide dismutase 1 with mutations linked to familial amyotrophic lateral sclerosis possesses significant activity. *Proceedings of the National Academy of Sciences of the United States of America* **91**, 8292-8296 (1994).
34 Robberecht, W. *et al.* Cu/Zn superoxide dismutase activity in familial and sporadic amyotrophic lateral sclerosis. *Journal of neurochemistry* **62**, 384-387 (1994).
35 Robberecht, W. *et al.* D90A heterozygosity in the SOD1 gene is associated with familial and apparently sporadic amyotrophic lateral sclerosis. *Neurology* **47**, 1336-1339 (1996).
36 Cleveland, D. W. & Rothstein, J. D. From Charcot to Lou Gehrig: deciphering selective motor neuron death in ALS. *Nature reviews. Neuroscience* **2**, 806-819, doi:10.1038/35097565 (2001).
37 Gurney, M. E. *et al.* Motor neuron degeneration in mice that express a human Cu,Zn superoxide dismutase mutation. *Science (New York, N.Y.)* **264**, 1772-1775 (1994).
38 Bruijn, L. I. *et al.* ALS-linked SOD1 mutant G85R mediates damage to astrocytes and promotes rapidly progressive disease with SOD1-containing inclusions. *Neuron* **18**, 327-338 (1997).
39 Howland, D. S. *et al.* Focal loss of the glutamate transporter EAAT2 in a transgenic rat model of SOD1 mutant-mediated amyotrophic lateral sclerosis (ALS). *Proceedings of the National Academy of Sciences of the United States of America* **99**, 1604-1609, doi:10.1073/pnas.032539299 (2002).
40 Ripps, M. E., Huntley, G. W., Hof, P. R., Morrison, J. H. & Gordon, J. W. Transgenic mice expressing an altered murine superoxide dismutase gene provide an animal model of amyotrophic lateral sclerosis. *Proceedings of the National Academy of Sciences of the United States of America* **92**, 689-693 (1995).
41 Wong, P. C. *et al.* An adverse property of a familial ALS-linked SOD1 mutation causes motor neuron disease characterized by vacuolar degeneration of mitochondria. *Neuron* **14**, 1105-1116 (1995).

42 Higgins, C. M., Jung, C. & Xu, Z. ALS-associated mutant SOD1G93A causes mitochondrial vacuolation by expansion of the intermembrane space and by involvement of SOD1 aggregation and peroxisomes. *BMC neuroscience* **4**, 16, doi:10.1186/1471-2202-4-16 (2003).
43 Fischer, L. R. *et al.* Amyotrophic lateral sclerosis is a distal axonopathy: evidence in mice and man. *Experimental neurology* **185**, 232-240 (2004).
44 Reaume, A. G. *et al.* Motor neurons in Cu/Zn superoxide dismutase-deficient mice develop normally but exhibit enhanced cell death after axonal injury. *Nature genetics* **13**, 43-47, doi:10.1038/ng0596-43 (1996).
45 Kanekura, K., Suzuki, H., Aiso, S. & Matsuoka, M. ER stress and unfolded protein response in amyotrophic lateral sclerosis. *Molecular neurobiology* **39**, 81-89, doi:10.1007/s12035-009-8054-3 (2009).
46 Ilieva, H., Polymenidou, M. & Cleveland, D. W. Non-cell autonomous toxicity in neurodegenerative disorders: ALS and beyond. *The Journal of cell biology* **187**, 761-772, doi:10.1083/jcb.200908164 (2009).
47 Lemmens, R., Moore, M. J., Al-Chalabi, A., Brown, R. H. & Robberecht, W. RNA metabolism and the pathogenesis of motor neuron diseases. *Trends in neurosciences* **33**, 249-258, doi:10.1016/j.tins.2010.02.003 (2010).
48 Buratti, E., Brindisi, A., Pagani, F. & Baralle, F. E. Nuclear factor TDP-43 binds to the polymorphic TG repeats in CFTR intron 8 and causes skipping of exon 9: a functional link with disease penetrance. *American journal of human genetics* **74**, 1322-1325, doi:10.1086/420978 (2004).
49 Buratti, E. *et al.* Nuclear factor TDP-43 and SR proteins promote in vitro and in vivo CFTR exon 9 skipping. *The EMBO journal* **20**, 1774-1784, doi:10.1093/emboj/20.7.1774 (2001).
50 Tollervey, J. R. *et al.* Characterizing the RNA targets and position-dependent splicing regulation by TDP-43. *Nature neuroscience* **14**, 452-458, doi:10.1038/nn.2778 (2011).
51 Kwiatkowski, T. J. *et al.* Mutations in the FUS/TLS gene on chromosome 16 cause familial amyotrophic lateral sclerosis. *Science (New York, N.Y.)* **323**, 1205-1208, doi:10.1126/science.1166066 (2009).
52 Sun, Z. *et al.* Molecular determinants and genetic modifiers of aggregation and toxicity for the ALS disease protein FUS/TLS. *PLoS biology* **9**, doi:10.1371/journal.pbio.1000614 (2011).
53 Bäumer, D. *et al.* Juvenile ALS with basophilic inclusions is a FUS proteinopathy with FUS mutations. *Neurology* **75**, 611-618, doi:10.1212/WNL.0b013e3181ed9cde (2010).
54 Huang, E. J. *et al.* Extensive FUS-immunoreactive pathology in juvenile amyotrophic lateral sclerosis with basophilic inclusions. *Brain pathology (Zurich, Switzerland)* **20**, 1069-1076, doi:10.1111/j.1750-3639.2010.00413.x (2010).
55 Waibel, S., Neumann, M., Rabe, M., Meyer, T. & Ludolph, A. C. Novel missense and truncating mutations in FUS/TLS in familial ALS. *Neurology* **75**, 815-817, doi:10.1212/WNL.0b013e3181f07e26 (2010).
56 Fujii, R. *et al.* The RNA binding protein TLS is translocated to dendritic spines by mGluR5 activation and regulates spine morphology. *Current biology : CB* **15**, 587-593, doi:10.1016/j.cub.2005.01.058 (2005).
57 Zinszner, H., Sok, J., Immanuel, D., Yin, Y. & Ron, D. TLS (FUS) binds RNA in vivo and engages in nucleo-cytoplasmic shuttling. *Journal of cell science* **110 (Pt 15)**, 1741-1750 (1997).
58 Hall, E. D., Oostveen, J. A. & Gurney, M. E. Relationship of microglial and astrocytic activation to disease onset and progression in a transgenic model of familial ALS. *Glia* **23**, 249-256 (1998).
59 Staats, K. A. & Van Den Bosch, L. Astrocytes in amyotrophic lateral sclerosis: direct effects on motor neuron survival. *Journal of biological physics* **35**, 337-346, doi:10.1007/s10867-009-9141-4 (2009).
60 Van Den Bosch, L., Van Damme, P., Bogaert, E. & Robberecht, W. The role of excitotoxicity in the pathogenesis of amyotrophic lateral sclerosis. *Biochimica et biophysica acta* **1762**, 1068-1082, doi:10.1016/j.bbadis.2006.05.002 (2006).
61 Maher, P. & Davis, J. B. The role of monoamine metabolism in oxidative glutamate toxicity. *The Journal of neuroscience : the official journal of the Society for Neuroscience* **16**, 6394-6401 (1996).
62 Hensley, K. *et al.* On the relation of oxidative stress to neuroinflammation: lessons learned from the G93A-SOD1 mouse model of amyotrophic lateral sclerosis. *Antioxidants & redox signaling* **8**, 2075-2087, doi:10.1089/ars.2006.8.2075 (2006).

63 van Blitterswijk, M. *et al.* Genetic modifiers in carriers of repeat expansions in the C9ORF72 gene. *Molecular neurodegeneration* **9**, 38, doi:10.1186/1750-1326-9-38 (2014).
64 Hawkes, N. A. *et al.* Purification and characterization of the human elongator complex. *The Journal of biological chemistry* **277**, 3047-3052, doi:10.1074/jbc.M110445200 (2002).
65 Otero, G. *et al.* Elongator, a Multisubunit Component of a Novel RNA Polymerase II Holoenzyme for Transcriptional Elongation. *Molecular Cell* **3**, doi:10.1016/S1097-2765(00)80179-3 (1999).
66 Q Svejstrup, J. Elongator complex: how many roles does it play? *Current Opinion in Cell Biology* **19**, 331336, doi:10.1016/j.ceb.2007.04.005 (2007).
67 Winkler, G. S., Kristjuhan, A., Erdjument-Bromage, H., Tempst, P. & Svejstrup, J. Q. Elongator is a histone H3 and H4 acetyltransferase important for normal histone acetylation levels in vivo. *Proceedings of the National Academy of Sciences of the United States of America* **99**, 3517-3522, doi:10.1073/pnas.022042899 (2002).
68 Okada, Y., Yamagata, K., Hong, K., Wakayama, T. & Zhang, Y. A role for the elongator complex in zygotic paternal genome demethylation. *Nature* **463**, 554-558, doi:10.1038/nature08732 (2010).
69 R. Björk, G., Huang, B., P. Persson, O. & S. Byström, A. A conserved modified wobble nucleoside (mcm5s2U) in lysyl-tRNA is required for viability in yeast. *RNA* **13**, 1245-1255, doi:10.1261/rna.558707 (2007).
70 Björk, G. R. *et al.* A primordial tRNA modification required for the evolution of life? *The EMBO journal* **20**, 231-239, doi:10.1093/emboj/20.1.231 (2001).
71 Aström, S. U. & Byström, A. S. Rit1, a tRNA backbone-modifying enzyme that mediates initiator and elongator tRNA discrimination. *Cell* **79**, 535-546 (1994).
72 Cusack, S., Yaremchuk, A. & Tukalo, M. The crystal structures of T. thermophilus lysyl-tRNA synthetase complexed with E. coli tRNA(Lys) and a T. thermophilus tRNA(Lys) transcript: anticodon recognition and conformational changes upon binding of a lysyl-adenylate analogue. *The EMBO journal* **15**, 6321-6334 (1996).
73 Ashraf, S. S. *et al.* Single atom modification (O-->S) of tRNA confers ribosome binding. *RNA (New York, N.Y.)* **5**, 188-194 (1999).
74 Krüger, M. K., Pedersen, S., Hagervall, T. G. & Sørensen, M. A. The modification of the wobble base of tRNAGlu modulates the translation rate of glutamic acid codons in vivo. *Journal of molecular biology* **284**, 621-631, doi:10.1006/jmbi.1998.2196 (1998).
75 Urbonavicius, J., Qian, Q., Durand, J. M., Hagervall, T. G. & Björk, G. R. Improvement of reading frame maintenance is a common function for several tRNA modifications. *The EMBO journal* **20**, 4863-4873, doi:10.1093/emboj/20.17.4863 (2001).
76 Smith, C. J., Teh, H. S., Ley, A. N. & D'Obrenan, P. The nucleotide sequences and coding properties of the major and minor lysine transfer ribonucleic acids from the haploid yeast Saccharomyces cerevisiae S288C. *The Journal of biological chemistry* **248**, 4475-4485 (1973).
77 Agris, P. F., Vendeix, F. A. & Graham, W. D. tRNA's wobble decoding of the genome: 40 years of modification. *Journal of molecular biology* **366**, 1-13, doi:10.1016/j.jmb.2006.11.046 (2007).
78 Agris, P. F. Wobble position modified nucleosides evolved to select transfer RNA codon recognition: a modified-wobble hypothesis. *Biochimie* **73**, 1345-1349 (1991).
79 Takai, K. & Yokoyama, S. Roles of 5-substituents of tRNA wobble uridines in the recognition of purine-ending codons. *Nucleic acids research* **31**, 6383-6391 (2003).
80 Lim, V. I. Analysis of action of wobble nucleoside modifications on codon-anticodon pairing within the ribosome. *Journal of molecular biology* **240**, 8-19, doi:10.1006/jmbi.1994.1413 (1994).
81 Yokoyama, S. *et al.* Molecular mechanism of codon recognition by tRNA species with modified uridine in the first position of the anticodon. *Proceedings of the National Academy of Sciences of the United States of America* **82**, 4905-4909 (1985).
82 Murphy, F. V., Ramakrishnan, V., Malkiewicz, A. & Agris, P. F. The role of modifications in codon discrimination by tRNA(Lys)UUU. *Nature structural & molecular biology* **11**, 1186-1191, doi:10.1038/nsmb861 (2004).
83 Huang, B., J.O. Johansson, M. & S. Bystrom, A. An early step in wobble uridine tRNA modification requires the Elongator complex. *RNA* **11**, 424-436, doi:10.1261/rna.7247705 (2005).

84 Chen, C., Huang, B., Eliasson, M., Rydén, P. & S Byström, A. Elongator complex influences telomeric gene silencing and DNA damage response by its role in wobble uridine tRNA modification. *PLoS genetics* **7**, doi:10.1371/journal.pgen.1002258 (2011).
85 Karlsborn, T. *et al.* Elongator, a conserved complex required for wobble uridine modifications in eukaryotes. *RNA biology* **11**, 1519-1528, doi:10.4161/15476286.2014.992276 (2014).
86 Chen, D. *et al.* Global transcriptional responses of fission yeast to environmental stress. *Molecular biology of the cell* **14**, 214-229, doi:10.1091/mbc.E02-08-0499 (2003).
87 Chen, D. *et al.* Multiple pathways differentially regulate global oxidative stress responses in fission yeast. *Molecular biology of the cell* **19**, 308-317, doi:10.1091/mbc.E07-08-0735 (2008).
88 Miśkiewicz, K. *et al.* ELP3 controls active zone morphology by acetylating the ELKS family member Bruchpilot. *Neuron* **72**, 776-788, doi:10.1016/j.neuron.2011.10.010 (2011).
89 Feil, R. *et al.* Ligand-activated site-specific recombination in mice. *Proceedings of the National Academy of Sciences of the United States of America* **93**, 10887-10890 (1996).
90 Hayashi, S. & McMahon, A. P. Efficient recombination in diverse tissues by a tamoxifen-inducible form of Cre: a tool for temporally regulated gene activation/inactivation in the mouse. *Developmental biology* **244**, 305-318, doi:10.1006/dbio.2002.0597 (2002).
91 Lemmens, R. *et al.* Overexpression of mutant superoxide dismutase 1 causes a motor axonopathy in the zebrafish. *Human molecular genetics* **16**, 2359-2365, doi:10.1093/hmg/ddm193 (2007).
92 Riboldi, G. *et al.* ALS genetic modifiers that increase survival of SOD1 mice and are suitable for therapeutic development. *Progress in neurobiology* **95**, 133-148, doi:10.1016/j.pneurobio.2011.07.009 (2011).
93 Van Hoecke, A. *et al.* EPHA4 is a disease modifier of amyotrophic lateral sclerosis in animal models and in humans. *Nature medicine* **18**, 1418-1422, doi:10.1038/nm.2901 (2012).
94 Van Damme, P., Dewil, M., Robberecht, W. & Van Den Bosch, L. Excitotoxicity and amyotrophic lateral sclerosis. *Neuro-degenerative diseases* **2**, 147-159, doi:10.1159/000089620 (2005).
95 Eisen, A. Amyotrophic lateral sclerosis: A 40-year personal perspective. *Journal of clinical neuroscience : official journal of the Neurosurgical Society of Australasia* **16**, 505-512, doi:10.1016/j.jocn.2008.07.072 (2009).
96 Chen, Y.-T. T. *et al.* Loss of mouse Ikbkap, a subunit of elongator, leads to transcriptional deficits and embryonic lethality that can be rescued by human IKBKAP. *Molecular and cellular biology* **29**, 736-744, doi:10.1128/MCB.01313-08 (2009).
97 Lumsden, A. L., Henshall, T. L., Dayan, S., Lardelli, M. T. & Richards, R. I. Huntingtin-deficient zebrafish exhibit defects in iron utilization and development. *Human molecular genetics* **16**, 1905-1920, doi:10.1093/hmg/ddm138 (2007).
98 Kabashi, E., Champagne, N., Brustein, E. & Drapeau, P. In the swim of things: recent insights to neurogenetic disorders from zebrafish. *Trends in genetics : TIG* **26**, 373-381, doi:10.1016/j.tig.2010.05.004 (2010).
99 Babin, P. J., Goizet, C. & Raldúa, D. Zebrafish models of human motor neuron diseases: advantages and limitations. *Progress in neurobiology* **118**, 36-58, doi:10.1016/j.pneurobio.2014.03.001 (2014).
100 Chen, Y. G. & Brushart, T. M. The effect of denervated muscle and Schwann cells on axon collateral sprouting. *The Journal of hand surgery* **23**, 1025-1033, doi:10.1016/S0363-5023(98)80010-5 (1998).
101 Son, Y. J. & Thompson, W. J. Nerve sprouting in muscle is induced and guided by processes extended by Schwann cells. *Neuron* **14**, 133-141 (1995).
102 Wittschieben, B. O. *et al.* A novel histone acetyltransferase is an integral subunit of elongating RNA polymerase II holoenzyme. *Molecular cell* **4**, 123-128 (1999).
103 Esberg, A., Huang, B., Johansson, M. J. & Byström, A. S. Elevated levels of two tRNA species bypass the requirement for elongator complex in transcription and exocytosis. *Molecular cell* **24**, 139-148, doi:10.1016/j.molcel.2006.07.031 (2006).
104 Karlsborn, T., Tükenmez, H., Chen, C. & Byström, A. S. Familial dysautonomia (FD) patients have reduced levels of the modified wobble nucleoside mcm(5)s(2)U in tRNA. *Biochemical and biophysical research communications* **454**, 441-445, doi:10.1016/j.bbrc.2014.10.116 (2014).